

JRC TECHNICAL REPORTS

Guidelines for harmonized vulnerability and risk assessment for non-nuclear critical infrastructure

STREST Reference Report 3

Editor: Iervolino I

Contributors: Anastasiadis A, Argyroudis S, Babič A, Basco A, Casotto C, Crowley H, Dolšek M, Fotopoulou S, Galbusera L, Giannopoulos G, Giardini D, Kakderi K, Karafagka S, Matos J P, Pitilakis K, Rodrigues D, Salzano E, Schleiss A J

Reviewer: Mignan A

Publishing editor: Tsionis G

2016



This publication is a Technical report by the Joint Research Centre (JRC), the European Commission's science and knowledge service. It aims to provide evidence-based scientific support to the European policymaking process. The scientific output expressed does not imply a policy position of the European Commission. Neither the European Commission nor any person acting on behalf of the Commission is responsible for the use that might be made of this publication.

JRC Science Hub

<https://ec.europa.eu/jrc>

JRC104650

EUR 28344 EN

PDF	ISBN 978-92-79-64606-5	ISSN 1831-9424	doi:10.2788/10912
Print	ISBN 978-92-79-64607-2	ISSN 1018-5593	doi:10.2788/984814

Luxembourg: Publications Office of the European Union, 2016

© European Union, 2016

The reuse of the document is authorised, provided the source is acknowledged and the original meaning or message of the texts are not distorted. The European Commission shall not be held liable for any consequences stemming from the reuse.

How to cite this report: Iervolino I, Anastasiadis A, Argyroudis S, Babić A, Basco A, Casotto C, Crowley H, Dolšek M, Fotopoulou S, Galbusera L, Giannopoulos G, Giardini D, Kakderi K, Karafagka S, Matos J P, Mignan A, Pitolakis K, Rodrigues D, Salzano E, Schleiss A J, Tsionis G, *Guidelines for harmonized vulnerability and risk assessment for non-nuclear critical infrastructure*, EUR 28344 EN, doi:10.2788/10912



D 7.6.3

DELIVERABLE

PROJECT INFORMATION

Project Title: Harmonized approach to stress tests for critical infrastructures against natural hazards

Acronym: STREST

Project N°: 603389

Call N°: FP7-ENV-2013-two-stage

Project start: 01 October 2013

Duration: 36 months

DELIVERABLE INFORMATION

Deliverable Title: Guidelines for harmonized vulnerability and risk assessment for non-nuclear critical infrastructure

Date of issue: 31 July 2016

Work Package: WP7 – Dissemination and stakeholder interaction

Editor/Author: Iunio Iervolino
(Analisi e Monitoraggio del Rischio Ambientale)

Reviewer: Arnaud Mignan
(ETH Zürich)

REVISION: Final



Project Coordinator: Prof. Domenico Giardini
Institution: ETH Zürich
e-mail: giardini@sed.ethz.ch
fax: + 41 446331065
telephone: + 41 446332610

Table of contents

1. Introduction	1
2. Taxonomy of the critical infrastructures	3
2.1 Summary of STREST classification of critical infrastructures	3
2.2 Vulnerability factsheets.....	5
2.3 Dependencies factsheets.....	5
3. Site-specific high consequence facilities	7
3.1 CI-A1: ENI/Kuwait oil refinery and petrochemical plant, Milazzo (IT)	8
3.1.1 Technological hazard.....	8
3.1.2 Vulnerability model	9
3.2 CI-A2: Large dams in the Valais region of Switzerland	11
3.2.1 Introduction	11
3.2.2 Vulnerability model	13
3.2.3 Vulnerability functions	14
3.2.4 Integrating the assumed vulnerability models.....	19
3.3 CI-B3 - Port infrastructures of Thessaloniki, Greece.....	21
3.3.1 Definition of limit damage states.....	21
3.3.2 Construction of fragility curves	22
4. Distributed critical infrastructures.....	25
4.1 CI-B1: Major Hydrocarbon Pipelines in Turkey	26
4.1.1 Vulnerability models.....	26
4.1.2 Performance and loss assessment.....	26
4.2 CI-B2: Gasunie National Gas Storage and Distribution Network in Holland	26
4.2.1 Vulnerability models.....	26
4.2.2 Performance and loss assessment.....	26
4.3 CI-B3: Port Infrastructures of Thessaloniki in Greece.....	27
4.3.1 Vulnerability models.....	27
4.3.2 Performance and loss assessment.....	27
5. Multiple-site, low-risk, high-impact, non-nuclear critical infrastructures	29
5.1 CI-C1: Industrial district, Italy	29
5.1.1 Structural and non-structural fragility.....	29
5.1.2 Contents fragility	31
5.1.3 Vulnerability models.....	32
5.2 Probabilistic multi-site loss modelling	32
6. Conclusions.....	35
References	37
List of abbreviations and definitions.....	43
List of figures.....	45
List of tables.....	47

Abstract

Loss assessment of critical infrastructures (CIs) subject to natural hazards is fundamental to stress tests. The systemic approach that lifelines require for performance modelling is an open research topic, given their logical and physical complexity. The Work Package 4 (WP4) of STREST focused on the guidelines for the vulnerability assessment of critical infrastructures categorized as:

- A Individual, single-site infrastructures with high risk and potential for high local impact and regional or global consequences;
- B Distributed and/or geographically-extended infrastructures with potentially high economic and environmental impact;
- C Distributed, multiple-site infrastructures with low individual impact but large collective impact or dependencies.

This reference report documents and summarizes the results of STREST WP4 via a series of applications and procedures (mostly referring to the seismic hazard case because of the level of advancement of research with respect to other natural hazards). The main attempt was to treat different CIs in a homogeneous framework derived and adapted from the well-known performance-based earthquake engineering developed for individual structures. From this effort it may be concluded that it seems possible to apply a unique logical framework to different CIs exposed to different natural hazards; nevertheless the performance/loss models for the key vulnerable components of each of them are still mostly lacking.

Acknowledgments

The research leading to these results has received funding from the European Community's Seventh Framework Programme [FP7/2007-2013] under grant agreement n° 603389.

Deliverable contributors

EUCENTRE	Helen Crowley Chiara Casotto Daniela Rodrigues
UL	Matjaz Dolšek Anze Babič
JRC	Luca Galbusera Georgios Giannopoulos
AMRA	Iunio Iervolino Ernesto Salzano Anna Basco
AUTH	Kyriazis Pitilakis Stella Karafagka Stavroula Fotopoulou Kalliopi Kakderi Sotiris Argyroudis Anastasios Anastasiadis
EPFL	José P. Matos Anton J. Schleiss

1. Introduction

Loss assessment of critical infrastructures (CI) subject to natural hazards has been one of the key tasks of the STREST project since loss susceptibility is one of the key attributes of resiliency (see Stojadinovic et al., 2016). Given that natural hazard (e.g., earthquakes, floods, tsunamis, etc.) assessment is somewhat consolidated to date, the main research needs are on CI vulnerability (e.g., response and consequence) modelling. In fact, while vulnerability assessment for individual structures (i.e., buildings) is also advanced, the systemic approach that lifelines require has not been fully addressed to date. This is why WP4 of STREST focused on the guidelines for the vulnerability assessment of CIs. Since each system logic requires a specific approach to the performance assessment, the CIs were categorized in three classes, as:

- A Individual, single-site infrastructures with high risk and potential for high local impact and regional or global consequences;
- B Distributed and/or geographically-extended infrastructures with potentially high economic and environmental impact;
- C Distributed, multiple-site infrastructures with low individual impact but large collective impact or dependencies.

Class A is the case of critical facilities (such as power plants) where the hazard has to be typically assessed for a point-like location, and the vulnerability of the facility requires to consider a system capable of domino and cascading effects, which may affect the community/area surrounding the facility. In these cases, direct damage is typically a negligible fraction of the loss while the triggered effects (e.g., an industrial accident) generate the main loss.

Class B is the case of the spatially-distributed infrastructures such as utility distribution networks. This kind of system needs hazard and vulnerability assessment reflecting the systemic (logically interconnected nature of the system) as well as its non-point-like spatial configuration (i.e., regional or multi-site hazard). For this type of systems, local failure may imply lifeline interruption for a large served community and downtime is usually the main cause of loss, even if locally there may be triggered accidents, for example because of hazardous material release, such as in gas distribution networks.

Finally class C is the typical case of building portfolios where individual hazardous events may trigger accumulated losses due to multiple (several) local failures and business downtime. The contemporaries losses in a building portfolio may be large such that the portfolio has to be considered as a critical infrastructure. The key example is that of industrial districts, where the individual components of the infrastructure are the individual industrial facilities.

This reference report provides practice-oriented guidelines for the performance and loss (i.e., vulnerability assessment) of CI typologies A to C via a series of exploratory applications/procedures. To this aim, the remainder of this document starts with the discussion of the taxonomy of CIs with respect to natural hazards. The taxonomy serves to list the key components for performance and loss assessment of each CI typology. Moreover, it serves to specify the required model for vulnerability assessment and the interfacing variables of these models. The interfacing variables link the vulnerability to hazard on one side (i.e., a natural event's intensity measure), and on the other side with the loss assessment (i.e., an engineering demand parameter to which associate damage). The taxonomy also serves to list the logical and physical dependencies of the components of the infrastructure with respect to the natural event considered. Subsequently, quantitative and standardized procedures and tools for consequence analysis are described for selected test cases of the three CIs' categories, putting more emphasis on those cases where new models have been developed by the STREST Project. In particular, a series of class A infrastructures are considered: (i) an oil refinery; (ii) a concrete dam; and (ii) a port infrastructure. Earthquake and tsunami hazards are those considered. Case (i) considers, as the main consequence, the possible

industrial accident triggered by the damage induced by a natural event, case (ii), the inundation eventually following structural failure of the dam, and case (iii), business interruption due to the port unavailability after a natural event. With respect to class-B CIs, the document mainly addresses seismic performance/loss assessment of distributed (utility) networks summarizing the results of previous large research efforts in this direction, which allowed to generalize the approach in the seismic case. The considered CI are distribution networks, which may be considered lifelines, as their downtime affects the served community (why the port infrastructure appears both in class A and B is briefly discussed at the beginning of chapter 3). Class C is addressed with respect to seismic hazard only and refers to a portfolio of industrial buildings constituting an industrial district. In this case, structural, non-structural, and content performance/loss modelling is key. Final remarks close the report.

2. Taxonomy of the critical infrastructures

2.1 Summary of STREST classification of critical infrastructures

The STREST project is covering three classes of critical infrastructures (CI):

- A Individual, single-site infrastructures with high risk and potential for high local impact and regional or global consequences;
- B Distributed and/or geographically-extended infrastructures with potentially high economic and environmental impact;
- C Distributed, multiple-site infrastructures with low individual impact but large collective impact or dependencies.

A number of case studies were considered for each of these CI classes, and despite their differences, they all share similar elements that are exposed to risk. In many cases, they include components from different systems, interacting to ensure the supply of the CIs' products and/or services. The STREST taxonomy describes (with a common language) the main components that are present in the following systems:

- Hydropower systems
- Electric power systems
- Waterfront components
- Earthen/rockfill embankments
- Roadway systems
- Railway systems
- Industrial warehouses
- Cargo handling / storage systems
- Fire-fighting systems
- Natural gas distribution and storage systems
- Oil refinery processing and storage systems
- Hydrocarbon distribution and storage systems
- Hydropower systems
- Liquid fuel systems
- Waste-water systems

STREST Deliverable 4.4 (2015) describes in detail the STREST taxonomy - that builds upon the taxonomy developed in the SYNER-G project (Hancilar and Taucer, 2013) - for classifying the individual components listed below that can be found within these different systems, such that each CI can be described in a harmonized way:

- Appurtenant structures
- Backup power (generator)
- Breakwaters
- Bridge abutments
- Bridges
- Buildings
- Building contents
- Compensation reservoir

- Cranes
- Distribution Circuits
- Electricity Lines
- Fire-hydrant
- Gas Pipelines
- Gravity Retaining Structures
- Mooring and Breasting Dolphins
- Oil / Gas Storage Tanks
- Oil Pipelines
- Other Pipelines
- Other Storage Tanks
- Piers
- Pipeline Station
- Power plant
- Pump equipment
- Pumping Station
- Pumping Plants
- Refinery process components
- Road pavements (ground failure)
- SCADA (Supervisory Control And Data Acquisition system)
- Sheet Pile Wharves
- Substations
- Switchyard
- Telecommunication centre
- Tracks
- Transmission lines
- Treatment plant
- Water Pipelines / Conduits
- Water Storage Tanks
- Water Tunnels

STREST Deliverable 4.4 presents each of the above components, the CI/system within which they can be found, and then two columns for the classification: the first provides a list of generic typologies, and the second gives a more detailed list of so-called classification parameters. Some elements (such as pumping stations or cranes) can be comprehensively described with a list of generic typologies, and sometimes this can be further expanded using some additional information that can be described using the classification parameters. Other elements (such as buildings and pipelines) instead have a very large number of potential typologies and so generic typologies are not available, and instead they require a classification system based on the classification parameters, such that ad-hoc typologies can be produced.

2.2 Vulnerability factsheets

Once the various components at risk were identified and described through the STREST taxonomy, the next critical step that was taken within the project was the identification of fragility/vulnerability characteristics of each component, and the intensity measure types needed to describe the hazards to which they are exposed. This information was collected through vulnerability factsheets that were compiled by the leaders of each case study, and which included the following information:

- Component needing a vulnerability model and its coordinates
- Hazard to which the component is vulnerable
- Primary Engineering Demand parameter (EDP1), i.e. most important parameter controlling structural response
- Secondary Engineering Demand parameter (EDP2) (if any)
- Limit States of interest and consequences of failure. What defines failure and undesired performance conditions triggering loss? Does the structure deteriorate in multiple events (e.g., aftershocks)?
- Primary preferred hazard intensity measure (IM1), i.e. most important analysis input parameter characterizing the potential of the natural hazard
- Secondary preferred hazard intensity measure (IM2) (if any)
- Site-specific or regional? Are IMs required at a single location or at multiple locations?
- If a vulnerability model for the component did not exist, the case study leaders had to clarify that it would be developed in the project?
- Stochastic modelling / uncertainty treatment in the model: What is the tool to address uncertainty in vulnerability of the component? E.g. Monte Carlo assessment, First Order Reliability Method etc.
- Analysis method for the performance assessment of the component: What method is used to evaluate vulnerability (e.g., analytical through non-linear dynamic analysis, empirical through observational data from other events...)?
- Interdependency: A preliminary assessment of whether the performance of the component is affected or affects other components of the same CI or of other CIs?

2.3 Dependencies factsheets

Inter- and intra-dependencies highly influence the performance of all kinds of complex facilities, as described in the dependencies factsheets provided in STREST Deliverable 4.4. A summary of the main outcomes of these factsheets is summarized below.

A survey of multiple dependencies of the CIs was carried out, accounting for the consequences of cascading failures and loss and availability assessment for supply-chains-like systems. Multi-infrastructure stress tests at a regional scale are performed on the basis of loss propagation and reciprocal impacts caused by failures. Dependencies eventually to be accounted for by the STREST approach and in the case study applications were thus identified. The factsheet includes a description of the existing intra-dependencies (between the components of each CI) and inter-dependencies (between the infrastructures of the CI and other networks) based on the SYNER-G project approach. Three different priority levels (i.e. crucial, important and secondary) and two types of interactions (i.e. direct and indirect) were considered. Crucial and important dependencies have been defined taking into consideration the methodology that will be implemented for their simulation. As a general remark, direct dependencies are in most cases classified at least as crucial and/or important. It is noted that only

interactions between components of different infrastructures and subsystems have been considered.

The most dependencies have been found in the hydrocarbon pipeline system in Turkey (HDRC), the harbour of Thessaloniki (HBR) and the Gasunie national gas storage and distribution network in Holland (GPN), where 110, 102 and 88 dependencies have been recognized respectively. For the large dams in Switzerland (DAM) and the oil refinery and petrochemical plant in Milazzo (REF), 64 and 31 dependencies have been provided, while the least dependencies (7) are defined in the industrial district in Italy (IDA).

In general, geographic (GEO) and physical (PHY) dependencies are the most common in all of the CIs. On the other hand, societal (SOC) and logical (LOG) interdependencies have not been defined in any CI. Restoration interactions (RES) are not present in the REF and IDA, while Sequential (Seq) dependencies are not present in DAM and IDA. Information (Inf) dependencies are identified only in HBR and HDRC, while general (Gen) ones are defined only in DAM and GPN.

This observation is related to the number of interacting assets that have been considered in each case, as in general, the ranking of dependencies per CI follows the amount of interacting components. However, the "dependency index" which here is defined as the ratio between the number of assets and the total number of dependencies in each CI, shows that the most dependent assets are in the industrial district (IDA), which is then followed by REF, DAM, HDRC, HBR and GPN. This is related to the way that each CI is working, the kind and number of different operations performed, as well as the number of components available to perform one task, e.g. the existence of redundant components minimizes the "dependency index".

Concerning the importance of priorities (in the framework of stress test), it is observed that HDRC has the most crucial dependencies, while HBR, GPN and IDA have less such dependencies. The most dependencies of second priority are defined in DAM and HDRC. On the other hand, HBR, GPN and HDRC have the most dependencies of third priority. This is related also in a way to the chosen approach of analysis for each CI, and the system operations that are of major importance to the whole system functionality and are going to be included in the methodology analysis framework.

Finally, in total, the most crucial dependencies (first priority) are the physical and geographic ones, while numerous geographic, physical dependencies are also considered in some cases as third priority dependencies, together with restoration dependencies. The "priority index", which here is defined as the ratio between the number of 1st, 2nd and 3rd priorities to the total number of dependencies for each type of interaction, shows that most of the dependencies are of 3rd priority. In particular, all the substitute (SUB) dependencies and most of the INF, Geo and Res dependencies are of 3rd priority. Such kind of interactions may in some cases have extremely adverse effects to the CI performance, and consequently to the served area, but since the subject of dependencies between CIs is rather a new research field, there are currently no available methods for their simulation and quantification.

3. Site-specific high consequence facilities

The Deliverable 4.1 has been specifically aimed at producing quantitative and standardized procedures and tools for the consequence analysis of two selected single-site CI classes, namely industrial CIs (CI-A1) and dams (CI-A2), starting from intensity measures/scenarios related to natural events produced in WP3 (see STREST European Reference Report 2).

The task was also intended to produce vulnerability functions for the selected CIs, from the component level (e.g., element-based-fragility) to the system level. The probabilistic vulnerability models accounted, if appropriate, for time-variant issues (e.g., aging and damage accumulation due to repeated shocks) in a consistent manner.

This report describes the main results of task 4.1 and is divided in three main parts, namely: T4.1-CI-A1: ENI/Kuwait oil refinery and petrochemical plant, Milazzo, Italy, followed by AMRA, T4.1-CI-A2: Large dams in the Valais region of Switzerland followed by EPFL, and T4.1-CI-B1: Port of Thessaloniki followed by AUTH. It is noted that while the CI-B1 is actually classified as distributed and/or geographically-extended infrastructures with potentially high economic and environmental impact (see Section 4), some of its components can be part of individual, single-site infrastructures (e.g. a single port pier), therefore, vulnerability functions produced for certain components (i.e. buildings and cranes) of the port system are presented in this section.

All the definitions and concepts described below use the same taxonomy as in Deliverable D4.4. Accident case studies and lessons learned from natural hazard impact on refineries, petrochemical plants, large dams and port areas can be found in STREST Deliverable D2.3 that discusses lessons learned from recent catastrophic events (Krausmann, 2011). For the three sections (CI-AI, CI-A2 and CI-B1) the proposed development may be sketched in three main steps and sub steps as reported in Fig. 3.1.

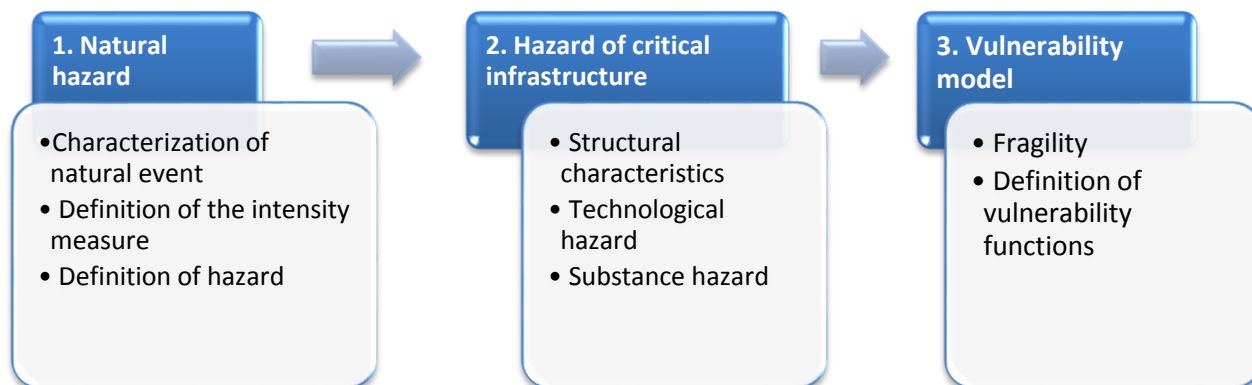


Fig. 3.1 The process flow for the vulnerability function developed in D4.1 for the single-site industrial equipment

Details on seismic hazard and near-source analysis can be found in Deliverable D3.3 of the STREST project. Tsunami Hazard is a measure of the potential for a tsunami to occur at a given site. More details can be found in Deliverable D3.1 of STREST project.

3.1 CI-A1: ENI/Kuwait oil refinery and petrochemical plant, Milazzo (IT)

3.1.1 Technological hazard

Within the chemical process industry, each equipment is characterised by different structural features and functions. In addition, any chemical process is intended to convert raw materials or intermediate products to final products. Hence, the hazard of the substance, during processing or storage, has to be evaluated, too. The primary sources that have the propensity to cause accidents can be determined either using the safety report of the plant or through existing risk assessment documentation. However, the selection of relevant hazardous equipment is an important step of the risk analysis procedure because it allows the reduction of the costs and time needed for the application of the method.

For the aims of this project, equipment have been categorized in three types with respect to the design standard: i) Atmospheric equipment (storage tank and process); ii) Pressurised equipment (cylindrical buried; cylindrical over-ground; spheres); and iii) Pipeline system. The following sections will be devoted to these three types of equipment only.

Atmospheric storage tanks are constructed worldwide based on API 650 (2015) and are geometrically characterised as vertical cylinder. Other atmospheric process equipment as distillation towers, separation units, or cyclones, are also designed with similar procedures however with slender geometry. For the structural point of view, all these types of equipment are generally built with carbon or stainless steel, with typical Maximum Allowable Working Pressure and corresponding failure pressure of few millibars. Shell thicknesses range from 5 mm to about 1 cm for some sections of jumbo tanks.

Pressurised equipment is often adopted for very hazardous substances and it is geometrically characterised as cylindrical (buried or over-ground) or spherical. The thickness, and the corresponding design pressure, are clearly larger than atmospheric equipment and may reach several centimetres for small equipment like chemical reactors.

Finally, the pipeline system within the installation may be aboveground or buried. Any release from natural-event triggered ruptures may result in a severe scenario. Pipelines may be continuous or segmented and are typically built from carbon or stainless steel when transporting hazardous or noxious substances.

Quite clearly, the technological hazard cannot neglect the hazards associated with the intrinsic chemical and physical hazards related to the processed or stored substances. Equipment items processing or storing flammable/toxic, highly flammable/toxic or extremely flammable/toxic substances according to the Classification, Labelling and Packaging Regulation (CLP-Regulation (EC) No 1272/2008), have surely to be considered as relevant sources of accidental events. Interestingly, studies have shown that earthquake-triggered structural damage involving water tanks is very similar to tanks containing hazardous materials and their behaviour can be described by a very similar methodology.

Besides, the physical state (gas, liquid, solid) and the operating conditions, which depend on the specific analysed process, are also of extreme importance. Eventually, a hazard matrix has been first developed and may be adopted for risk assessment (Table 3.1).

Table 3.1 Technology hazard matrix. 1: low - 4: high

	Liquefied gas	Overheated Liq	Gas	Cryogenic liq	Liquid
Pressurised	4	3	3	2	1
Atmospheric	4	3	2	2	1
Pipeline	3	2	2	2	1

This result may be used for prioritizing the case study and the consequence assessment, as described in the Quantitative Risk Analysis developed in Deliverable D5.1 of the STREST project, but must be crossed with the chemical hazard.

To this aim, the REACH Regulation (the Regulation on Registration, Evaluation, Authorisation and Restriction of Chemicals of the European Union, adopted to improve the protection of human health and the environment from the risks that can be posed by chemicals) is useful, if added to the information given by the Seveso Directives (e.g. Dir 2012/18/EU of the European Parliament and of the Council of 4 July 2012 on the control of major-accident hazards involving dangerous substances, amending and subsequently repealing council directive 96/82/EC) and with CLP (Guidance to Regulation (EC) No 1272/2008 on classification, labelling and packaging (CLP) of substances and mixtures, Version 4.1, June 2015, ECHA-15-G-05-EN). Indeed, the CLP informs on the hazard characteristic for any substance, and the Seveso Directives includes a list of chemicals and related threshold amount to consider the same chemicals as dangerous for workers, population and environment.

3.1.2 Vulnerability model

In the framework of a performance-based analysis related to natural events, damage should be classified according to fixed levels, generally called Damage States. For instance, HAZUS (HAZUS-MH MR4, 2009) provides the Damage States for many types of structures, components and groups of structures. Each Damage State DS is related to synthetic and representative intensity measures of the observed natural hazard.

In the case of NaTech analysis, different limit states related to the loss of containment from the given equipment, rather than structural vulnerability, need to be developed. These limit states are often defined as Risk State RS in the existing literature (Campedel et al., 2008; Salzano et al., 2009).

For each damage or risk state, a vulnerability function has been defined based on earthquake or tsunami intensity parameters. These functions have been retrieved from scientific literature or, if not existing, directly developed within the STREST project. The vulnerability functions were adopted in existing tools for the quantitative risk assessment and for the scope of CI-A1 task.

When equipment is designed, any good engineering practice takes into account the possible impact of natural events like snow, wind or earthquake. Some requirements for structural response of equipment when subjected to earthquakes are e.g. compulsory in early design phases.

With reference to the specific case of construction of atmospheric storage tanks, for instance, API 650 (2015) takes into account two response modes, for either anchored or unanchored tanks, with respect to earthquakes: a high frequency response to lateral ground motion of the liquid contents that moves in unison with shell, and a relatively low-frequency response of the liquid tank content that moves in the fundamental sloshing mode. The two modes lead to an overturning action of the tank.

Quite clearly, structural engineers can use more complex methodologies as Finite Element Analysis (see e.g. Eurocode 8 (EN 1998-1, 2003)). These tools are technically and economically sustainable only when a single case is considered or when designing

new equipment with important impacts on economy, but they become hard to be adopted when performing risk analysis of large installations or for industrial areas (parks), with many equipment items to be analysed.

To this regard, it is worth noting that the cited structural design codes or more simplified methodologies often do not take into account active or passive prevention and mitigation systems and are always addressed to the structural integrity (that is, to avoid the collapse of the structure) of the item, hence they do not take into account the integrity of connections or of piping. Indeed, the main aim of early phase design is typically the loss of serviceability and economic issues for system recovery, whereas few concerns are related to NaTech accidental scenarios, which may possibly involve the population and environment located in the surrounding of industrial installation. Eventually, these methodologies are not applicable to quantitative risk assessment of large industrial installations and the use of simplified empirical equipment vulnerability models based on observational data is necessary. Besides, the number of test cases to develop from the natural event to the possible scenarios (fire, explosion, dispersion of toxic substances), combined with the elevated number of equipment does not allow the use of even simple numerical lumped parameter models or distributed parameter models except with large economic and time efforts.

In the development of such tools, the damage classification proposed by HAZUS guideline (HAZUS-MH MR4, 2009) might be adopted and extended to any natural event in the framework of NaTech risk assessment. More specifically, limit states for structural damage (damage state, DS) may be defined for structural damages, though with specific reference to industrial purposes. According to HAZUS damage classification (1997), slight damages to structures have been defined as DS2, moderate damages as DS3, extensive damages as DS4 and total collapse of structure as DS5. The term DS1 refers to insignificant damage.

As suggested in the previous section, the framework of industrial risk assessment suggests however the adoption of an even more simplified approach based on a limited number of discrete damage states (DS). In the present document and with the aim of vulnerability ranking, a lower number of damage states needs to be identified as a possible consequence for any equipment loaded by an earthquake (Campedel et al., 2008; Salzano et al., 2009). The definition of DS will be given for each specific equipment in the following.

Furthermore, in quantitative risk assessment, "Risk States" (RS) have to be defined in order to obtain a measure of the quantity and rate of hazardous substances released from containment systems, following the structural damage of industrial equipment (Salzano et al., 2003; Salzano & Cozzani, 2007; Campedel et al., 2008) due to the impact vector characterizing the natural event.

As in the case of DS, also RS may vary between the total absence of release and the moderate release of hazardous substance, up to the extensive loss of containment. Quite clearly, the significance of RS may depend strongly on the equipment and substance type. In the case of pressurized equipment containing toxic substances, for instance, the consequences of both moderate and extensive release may be quite similar, because – due to pressurisation – even relatively small failures of shell structure may produce large damage and similar loss of containment (which depends only on loss section, due to choking flow). For any RS value, a correspondent accident scenario (fire, explosion, and toxic dispersion) may be associated. This passage is not described in this deliverable and is part of the more general application of quantitative risk assessment.

The damage state DS and the risk state RS can be correlated by simple analysis, which depends on the specific equipment type. Furthermore, starting from the definitions, industrial equipment vulnerability may be defined by correlating the intensity of the impact vector for the specific natural event to the probability of a given limit state (RS), for each category of equipment, by means of "fragility" curves:

$$P[RS \geq RS_i | IM] = \Phi \left[\frac{\ln(IM) - \mu}{\beta} \right] \quad (3.1)$$

where Φ is complementary cumulative normal distribution function, μ and σ are lognormal mean and standard deviation values, and IM is the intensity measure, i.e. the specific value of severity parameter that characterizes the natural event.

Eventually, for the generic natural event, given the equipment category (e.g. atmospheric or pressurized), we can define a NaTech vulnerability function P for each RS state as:

$$P[RS \geq RS_i | IM] = \int_{IM} P[RS \geq RS_i | IM] \cdot h(IM) dIM \quad (3.2)$$

In other terms, the marginal RS probability of any equipment conditional to the occurrence of event may be assessed by considering the corresponding hazard h of the natural event. The annual rate of RS exceedance is then computed by using the annual rate of occurrence.

Cost/benefit analysis and time effectiveness lead always to the introduction of strong simplifications in the analysis in order to obtain suitable tools for risk assessment. An even more simplified approach may be required when vulnerability ranking is needed.

Threshold values for the natural intensity $IM_{nat,thresh}$ may be useful, for any RS defined above, in order to produce a univocal value of the natural hazard severity for the sake of prioritisation of different equipment and process systems. To this aim, the use of probit analysis is normally adopted for their mathematical definition. Details of the procedure for probit analysis are reported elsewhere (Finney, 1971).

3.2 CI-A2: Large dams in the Valais region of Switzerland

3.2.1 Introduction

Regardless of their specific characteristics, which may vary markedly from case to case, large dams typically operate by storing substantial volumes of water in their upstream reservoir. The release of that water to downstream areas is normally controlled according to operational guidelines and targets. In view of that, in order to correctly frame risk and vulnerability assessments for dams, one should consider, beyond the dam body, the reservoir, the appurtenant structures (e.g. spillways, bottom outlets, or hydropower systems) and, most importantly, the downstream areas potentially affected by floods.

In fact, following a dam failure, typically characterized by an uncontrolled release of the reservoir, a large amount of water travels downstream in the form of a dam-break wave. Such waves travel extremely fast and have enormous eroding power, as well as transport capacity. The impact that a dam failure may have is dependent on a number of factors, perhaps more relevantly failure mechanism, volume of the reservoir, height and type of dam, the occupation of land downstream, and the exposure of the population to the dam-break wave. Despite these dependencies, impacts are generally acknowledgeable.

Large dams have historically led to a small number of catastrophic disasters. With failures taking place in well-defined locations – the dam body or even specific sections of it – the death toll of the worst dam failures ranged from hundreds to staggering numbers of tens of thousands of people (i.e. Banqiao embankment dam, Ru River, Henan Province, China, August 1975; the number of direct and indirect victims is believed to range from 30000 to some unfathomable 230000). The localized nature of the failures along with the significant consequences they may have justify that large dams are classified as critical infrastructures of class A.

Most countries promote a deterministic approach to dam safety assessment. Designers' focus is placed in large measure on structural responses and hydraulic behaviours, which are nowadays predicted with great accuracy. Dams, like many other complex systems, can be vulnerable to unforeseen combinations of relatively common events, either independently or following a major hazard, bringing about a failure. Not all of these events are necessarily captured by the deterministic approach; there is an advantage in moving towards and increased reliance on probabilistic frameworks. This section advocates for that.

On one hand, the implementation of probabilistic frameworks is not directly compatible with the use of detailed numerical models – these take much too long to run in order to be used in the large number of cases necessary to support a probabilistic analysis. On the other hand, the preparation and use of detailed numerical models adapted to the specific large dam under study is necessary and should not be abandoned. Indirect ways of combining both are needed.

Recognizing that the dam-reservoir system is intrinsically dynamic and subject to numerous interactions between different components of the dam, the reservoir, and hazards, a probabilistic framework based on the Generic Multi-Risk (GenMR) framework (Mignan et al. 2014) aimed to assess the overall risk associated with a conceptual large alpine embankment dam operating for a period of one year. In other words, beyond looking at isolated sources of risk or reference scenarios, this methodology sought to gain insight on the role of hazard interactions and the dynamical nature of the system. It was proven effective at that and, it is believed, may be a valuable asset in the vulnerability assessment of large dams.

The study of the dam-reservoir system and how failures can be brought about is undoubtedly important. Also extremely relevant is to assess what are the consequences to downstream areas once a dam-break wave is released. It is thus recommended that vulnerability assessments for large dams rely on probabilistic frameworks that successfully come to terms with the complexity and dynamic nature of a typical dam-reservoir system but, at the same time, handle the uncertainty that shrouds the downstream impacts of failures and the vulnerability of activities, land uses and populations to dam-break waves (Fig. 3.2).

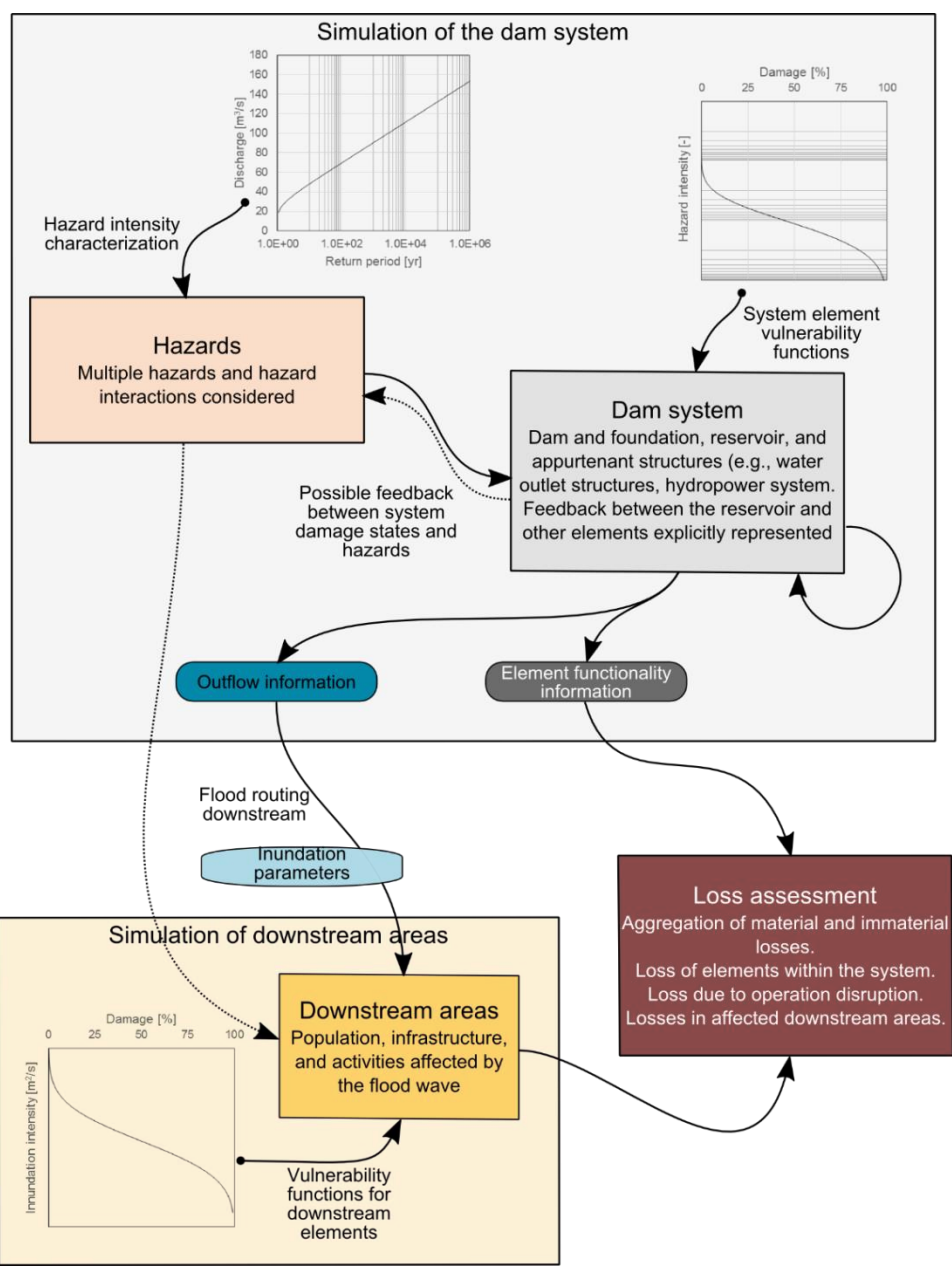


Fig. 3.2 Proposed framing of vulnerability and loss assessment for large dams. The analysis of potentially affected areas is downstream adds to the simulation of the dam system. The relationship between both "blocks" is achieved through flood wave routing.

3.2.2 Vulnerability model

Damage states

Although an element's integrity can range anywhere from 0 to 100%, particular damage states considered for CI-A2 were focused on the dam and foundation element and spillway. They are a gross simplification of what should be done for a real vulnerability assessment study of a large dam and were used in order to test the potential of the GenMR probabilistic framework with applied to this type of infrastructures. Functionality of hydraulic elements was assumed to be proportional to their integrity, down to a chosen threshold below which the element is considered inoperable (in practical terms it cannot be used to regulate reservoir levels).

Assuming that, at 50% integrity, the dam is no longer capable of holding the reservoir, damage states were quantified as follows:

- Dam not damaged: integrity between 95 and 100%,
- Dam mildly damaged: integrity between 90 and 95%,
- Dam tolerably damaged: integrity between 80 and 90%,
- Dam severely damaged: integrity between 70 and 80%, and
- Dam critically damaged: integrity between 50 and 70%.

The spillway was associated with a single damage state – spillway severely damaged – that corresponds to integrity below 85%. Below this level, the spillway was considered inoperable. Not damage states per se, but relevant nonetheless, are the integrity thresholds below which the remaining outflow structures are assumed not to function. These amount to 90%, for the bottom outlet, and 50% for the hydropower system.

Risk states

Risk states aim to represent undesired outcomes of a certain hazard or a combination of previous events. Firstly, the issue of a drawdown order is represented; it signals the attempted reduction of the reservoir level by all means necessary in order to prevent eventual further damage to the dam. Drawdown orders were assumed to be issued if the dam is either severely or critically damaged or the spillway is severely damaged. Secondly, the occurrence of moderate and “full” overtopping failure modes was rendered possible. Moderate overtopping occurs when the water level over the crest is marginal (lower than 50 cm on a limited section of the crest) and, although the dam endures some damage, a full breach is not necessarily developed. In opposition, “full” overtopping implies the failure of the dam. Finally, failures can be a consequence of damage accumulated by the dam and foundation that is not always linked to overtopping. Other hazards that may lead it are, for example, earthquakes or internal erosion. Knowing the cause of failure is relevant for outflow hydrograph estimations.

3.2.3 Vulnerability functions

Earthquakes

Vulnerabilities to earthquakes for the different elements considered in the dam-reservoir system are depicted in the next figures. Again, these constitute a gross simplification of best-practices and follow an inverse reasoning that assumes compliance to Swiss regulations. In a real study where a probabilistic framework is resorted to, it is recommended that vulnerability functions are derived from detailed numerical models; the specificity and importance of most large dams should more than justify custom modelling work.

As embankment dams are recognized to be particularly resilient to earthquakes, it was assumed that a 10 000 year return period earthquake would damage the structure without prompting the release of the reservoir, finally failing for a return period of approximately 1 000 000 years. Resorting to a similar reasoning, the spillway’s vulnerability was defined such that, for a 10 000 year return period earthquake, it remains functional while, for a 475 years return period event, it withstands little damage. Given the range of different building solutions for spillways, it is also recommended that these elements’ vulnerabilities are individually evaluated prior to practical applications of the methodology.

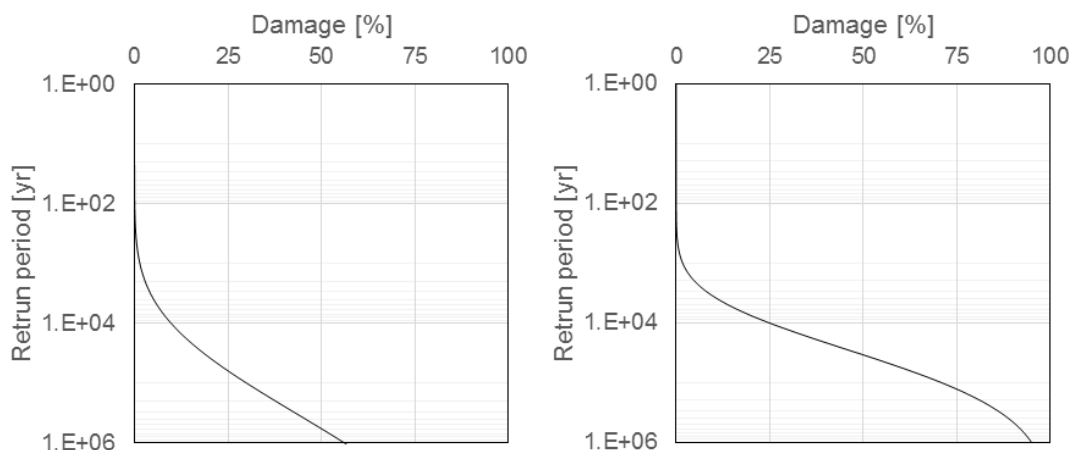


Fig. 3.3 Vulnerability curve of the dam and foundation (left) and of the spillway element (right) to earthquakes

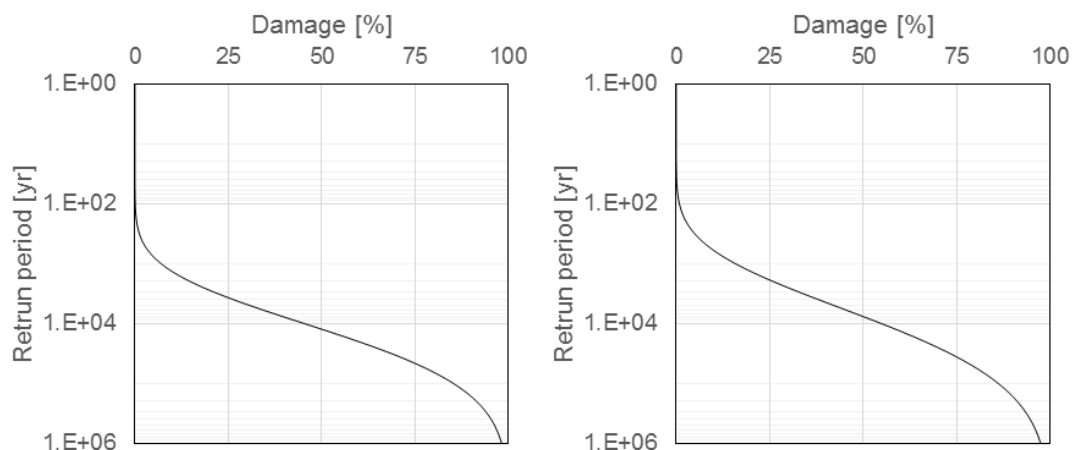


Fig. 3.4 Vulnerability of the bottom outlet element (left) and of the hydropower system (right) to earthquakes

The bottom outlet and hydropower systems, including mechanical equipment, were modelled as being more vulnerable to the earthquake hazards than the spillway, particularly due to the risk of gates jamming. Again, there was little information found in literature that contributes to the quantification of the vulnerabilities of such elements to earthquakes. The parameters of the applied log-normal curves, applied to PGA, are shown in Table 3.2. Stemming from earlier discussion, numbers such as these should be calculated specifically for every large dam.

Table 3.2 Parameters of the log-normal vulnerability functions to earthquakes (PGA). Specific for the conceptual dam system under study

Element	Location parameter (μ)	Shape parameter (σ)
Dam and foundations	-2	0.23
Spillway	-1.85	0.18
Bottom outlet	-1.95	0.19
Hydropower system	-1.6	0.29

Internal erosion

Only the dam and foundation element are considered vulnerable to internal erosion events. Internal erosion is a process which, after initiated, tends to develop very fast. In fact, as the more of the dam's material gets eroded, less resistance there is to the flow. This leads to more water exiting the dam body and ever more material being eroded, ultimately leading to a full breach being formed.

Due to this progressive behaviour, which is likely – but not guaranteed – to end in a failure of the dam, it is not straightforward to specify the hazard's intensity measure and corresponding vulnerability function. As such, the intensities that were used to characterize the hazard are assumed to be proportional to the damage endured by the structure. The curve is particularly steep in order to capture the evolving nature of the hazard, but although based in engineering judgement, its applicability is admittedly debatable and should be the target of further investigation. The admitted parameters for this log-normal were μ of -12 and σ equal to 1.

Equipment malfunction

The equipment malfunction hazard affects the bottom outlet and hydropower system. It represents the possibility of gates being jammed, under maintenance, or inoperable due to motor failures. Unlike for the previous vulnerabilities, damages associated with equipment malfunction are limited, as neither of the systems are expected to be completely destroyed by such an event. The proposed functions, based on statistics for mechanical equipment failure rates (Pohl, 2000), are depicted in Fig. 3.5 and detailed in Table 3.3. It should be stated, however, that such failure rates are heavily dependent on maintenance efforts and operability checks and, thus, are expected to vary widely between countries and even between dam operators.

Moderate overtopping

Finally, the vulnerability of the dam to moderate overtopping was modelled as a uniform random variable, being that for every moderate overtopping event it suffers a damage of 5 to 20%.

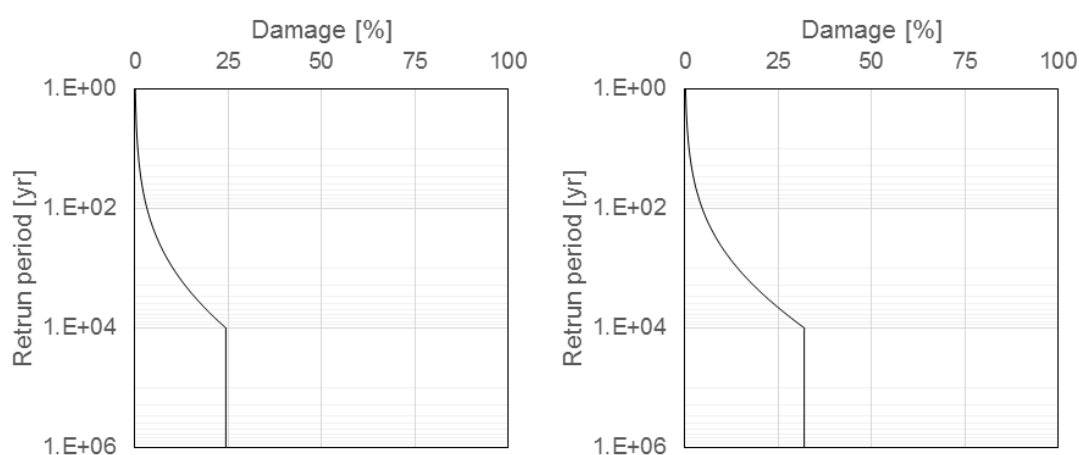


Fig. 3.5 Distribution of the damage induced to the bottom outlet element by equipment malfunction (left) and to the hydropower system by equipment malfunction (right)

Table 3.3 Parameters of the log-normal vulnerability functions to malfunctions. Specific for the conceptual dam system under study

Element	Location parameter (μ)	Shape parameter (σ)	Cut-off value (damage, %)
Bottom outlet	-12	4	25
Hydropower system	-11	3.8	30

Downstream structures and infrastructure

The vulnerability of downstream structures and infrastructures was modelled on the basis of inundation parameters. Unfortunately, there is little published information on the specific vulnerability of buildings to dam-break waves. As such, in the scope of this problem, vulnerabilities are based on publications made for natural floods and tsunamis, the latter particularly interesting as they are expected to – similarly to dam-break waves – carry a large amount of debris and travel fast.

Inundation depth

There is a plethora of different potential sources for vulnerability functions to floods based on inundation depth. Notably the Hazus-MH software (Department of Homeland Security Division Federal Emergency Management Agency Mitigation Division 2006), includes over 700 functions adapted to different buildings and contents, vehicles, etc.

As put forward above, however, dam-break floods differ from natural ones in several aspects and, perhaps, a better proxy for damages associated with dam-break waves results from vulnerabilities derived for the tsunami hazard. In addition, vulnerability functions depend on the building practises in each country and are marked by great uncertainty, varying widely among publications (e.g. de Moel & Aerts, 2011). Adequate vulnerability functions for Switzerland were not found.

An example of vulnerability functions specific for tsunamis derived from the project SCHEMA following the 2004 Indian Ocean tsunami (Tinti et al., 2011). Beyond the vulnerabilities derived in the scope of SCHEMA, a wealth of information on the fragility of buildings to tsunami action ensued from the 2011 Great East Japan tsunami (Suppasri et al., 2013). Fragility curves published from reinforced concrete structures were employed on the present case study. The curves derived by Suppasri et al. (2013) for two-story reinforced concrete buildings are illustrated in Fig. 3.6 for six damage classes. These are:

- a) Minor damage;
- b) Moderate damage;
- c) Major damage;
- d) Complete damage;
- e) Collapsed;
- f) Washed away.

Additionally to presenting curves for several types of building material and height, the authors highlight that building height plays an important role in observed damages, with constructions with more than three stories much less likely to be washed away, regardless of the building material.

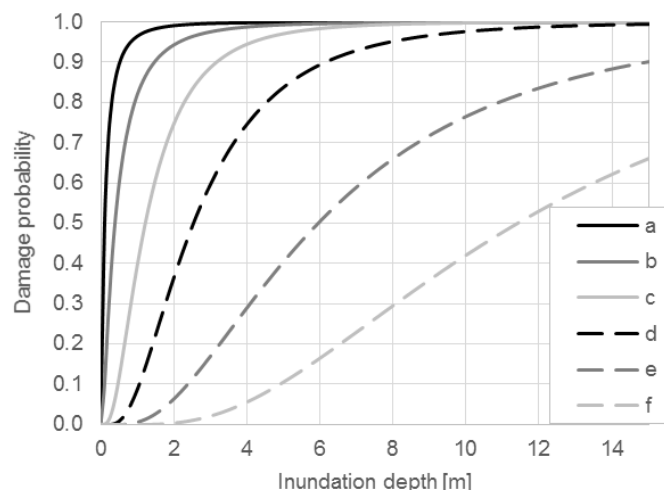


Fig. 3.6 Fragility curves derived by Suppasri et al. (2013) for two-stories reinforced concrete buildings.

Flow velocity

While water height is relatively easy to assess following a flood event, water velocity is more difficult to estimate. Partly due to this, the vast majority of flood-related vulnerability and fragility curves are based on the former. According to Kreibich et al. (2009), however, although water height constitutes a good predictor of structural damage to residential buildings, flow velocity works better as an independent variable for assessing damages to road infrastructure.

Even for buildings, it can be argued that accounting for flow velocities is important. In fact, for natural floods, the estimation of damages based on inundation depth alone implicitly assumes that either flow velocities remain below levels that pose a risk of structural damages or that flow velocity behaves as a function of water height. Dam-break waves can attain flow velocities that largely surpass those of natural floods and display highly unsteady behaviour, with steep rise and descent of water levels. Consequently, none of the implicit assumptions can be applied to them.

As an example, for the current case study and making use of only a fraction of the simulated data one can see that, although a correlation between simulated inundation depth and flow velocity indeed appears to be clear, there is ample scattering of the results (Fig. 3.7). Because no fragility curves were found for road infrastructure affected by dam-break waves or tsunamis, four fictitious fragility curves were assumed in order to test the model (Fig. 3.8 and Table 3.4). These correspond to minor (a), moderate (b), major (c), and complete damage (d).

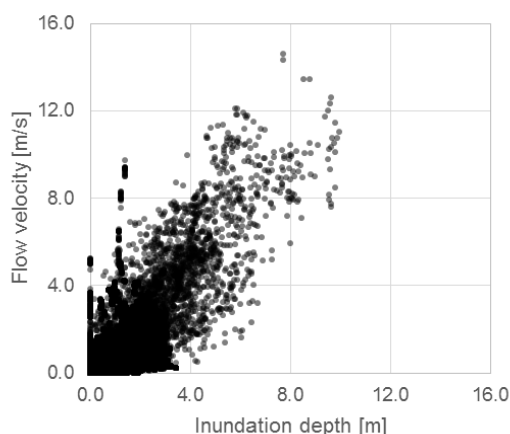


Fig. 3.7 Scatter plot depicting inundation depths and flow velocities simulated by a 2D model applied to the dam-break problem

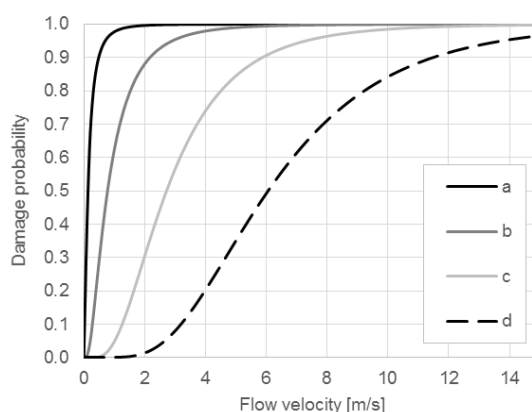


Fig. 3.8 Fragility curves admitted for road infrastructure

Table 3.4 Parameters of the log-normal fragility curves admitted for road infrastructure. Have been admitted solely for the purpose of illustrating the methodology

Damage state	Location parameter (μ)	Shape parameter (σ)
A	-2	1
B	-0.25	0.8
C	-1	0.6
D	1.8	0.5

3.2.4 Integrating the assumed vulnerability models

All described vulnerabilities were integrated after performing millions of simulations of the dam-reservoir system using the GenMR framework. Downstream impacts were assessed by a number of detailed numerical hydraulic simulations of the valley below the dam with a 1D-2D coupled model (BASEMENT, Vetch et al. 2005). Because each of these simulations takes hours to complete – that being hardly compatible with a probabilistic framework – machine learning models were used to derive inundation parameters at any place of the valley as a function of the dam’s outflow. Examples of the results obtained from the application of the methodology to buildings and roads are shown in Fig. 3.9 and Fig. 3.10.

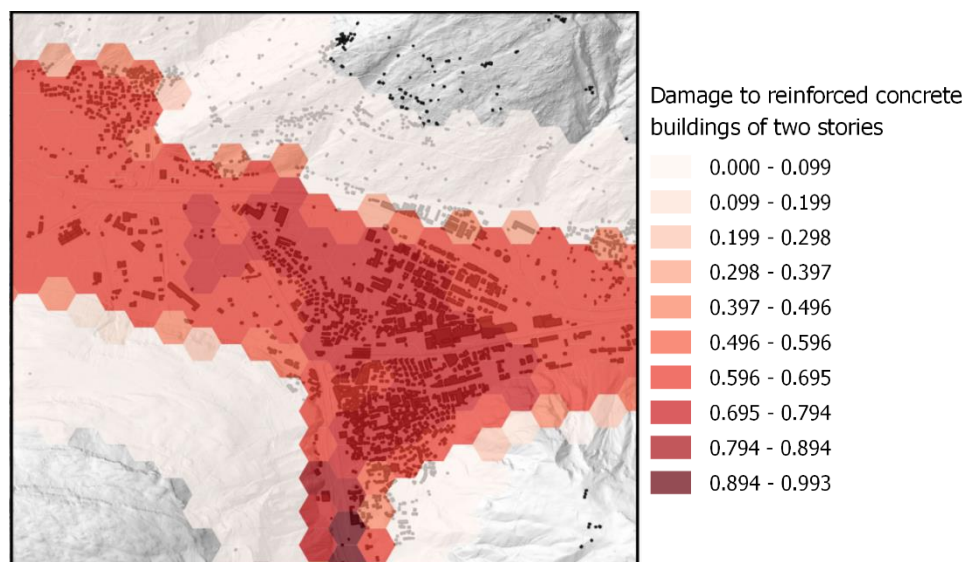


Fig. 3.9 Map of damages to reinforced concrete buildings of two stories corresponding to a specific dam-break event. Adapted from Salzano et al. (2015).

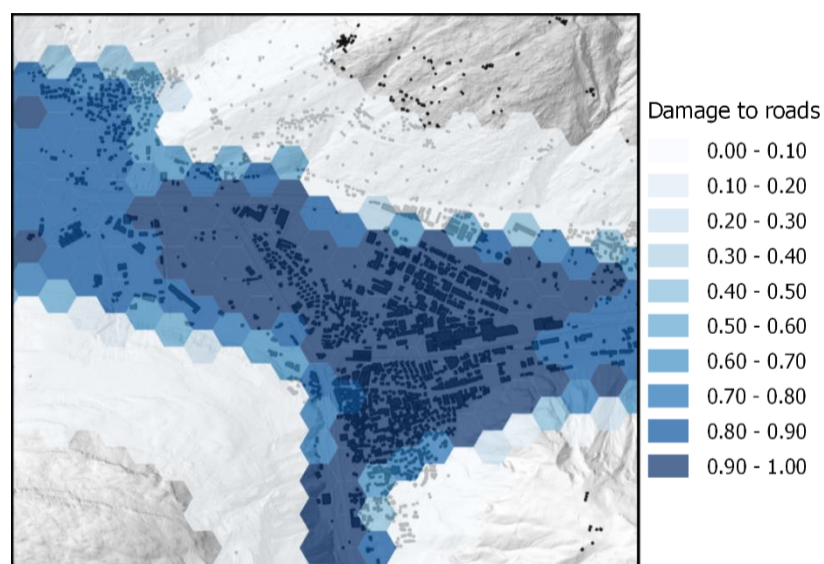


Fig. 3.10 Map of damages to roads corresponding to a specific dam-break event. Adapted from Salzano et al. (2015).

Through this work it was shown that probabilistic frameworks can be used with a number of advantages, particularly in what concerns the information that can be gotten by disaggregating results and the effects of uncertainty.

The novelty of the work and the added value of its recommendations are not bound to the vulnerability functions that were used or the depth to which specific processes have been handled. It is, in fact, quite simple in both regards and admittedly less elaborate than what best practices recommend for real-case studies. The novelty of what was done lies in the way in which the dynamical nature of the dam-reservoir system was modelled and in the fact that it successfully depicted interactions developed among a number of different hazards and system states. Also, it invested in transposing probabilistic results downstream and thus embracing the non-linearity of the vulnerabilities of buildings and roads to dam-break waves.

Finally, the work this section builds upon came short of studying loss of live. In what dam failures are concerned that is perhaps the most important aspect to define.

Although loss of life due to dam failures continues to be difficult to estimate and, therefore, does deserve additional study, here a conscious decision was made to contribute towards the parts of dam safety analysis that forcibly come before estimating how many lives may be lost in the event of a failure. Better knowledge of failure rates and their predominant mechanisms, as well as added insight on the estimation of inundation parameters such as maximum water depths, peak flow velocities, and time of arrival of the flood will certainly contribute to improved loss of life estimates.

3.3 CI-B3 - Port infrastructures of Thessaloniki, Greece

3.3.1 Definition of limit damage states

The definition of realistic limit damage states is of paramount importance for the construction of fragility curves. The selection of appropriate engineering demand parameters (EDP) to correlate with the selected IM (inundation depth) is a challenge, as a suitable EDP has not yet been established in literature. When a building response to tsunami comprises structural damage, damage states can be classified using the same schemes used for structural damage triggered by an earthquake (Bird et al. 2005). However, the use of a global damage index such as the interstorey drift is not appropriate to be used as a tsunami EDP as the expected deformed shape and damage mechanism of the structure impacted by a tsunami is quite different from that of the same structure subjected to ground shaking. Thus, a local damage index in terms of building's material strain can be used as it shows an improved correlation with structural damage (Macabuag et al., 2014). Four limit damage states (LS1, LS2, LS3 and LS4) are defined based on nonlinear static analyses (both seismic pushover and tsunami time history analyses) for the various typologies of the buildings and the crane, engineering judgment and the available literature (e.g. HAZUS-MH (2009), FEMA (2004), Crowley et al. (2004), Fotopoulou and Pitilakis (2013a; 2013b)). They describe the exceedance of minor, moderate, extensive and complete damage of the structures. According to FEMA (2004), "Steel Light Frames" structures are mostly single story structures combining rod-braced frames in one direction and moment frames in the other. Due to the repetitive nature of the structural systems, the type of damage to structural members is expected to be rather uniform throughout the structure. Consequently, warehouses are considered as "Steel Light Frames" structures. The limit state values finally adopted are presented in Table 3.5 and Table 3.6.

In order to minimize the uncertainties associated with the selection of the appropriate damage state limits, nonlinear static analyses including seismic pushover and tsunami time history analyses were performed for the different analysed structures to define structure-specific limit state values (in terms of strains) for each damage state.

Regarding the RC buildings, first a seismic pushover analysis was conducted to obtain a preliminary estimation of the damage states defined on the capacity curve. An iterative procedure followed to derive, for each damage limit state, the steel and concrete strains, which yield the corresponding roof displacement on the curve. It was seen that for all analysis cases, steel strain (ϵ_s) gives more critical results. Hence, hereafter, the proposed limit damage states were defined in terms of steel strain. In particular, for the MRF models with bare frames the first limit state was specified as steel bar yielding while for the infilled ones the infills cracking was assigned as the first limit state and steel bar yielding as the second one. For the rest limit states, mean values of post-yield limit strains for steel reinforcement are suggested. For the dual models, the steel strain limits considered in MRF models cannot be used to characterize the extensive and complete damage of the dual systems, as they lead to lower levels of top displacement on the capacity curve. Thus, increased values of steel strain limits were adopted. It should be noted that the behaviour of the dual models when considering or not infills does not change considerably. This is to be expected considering that the contribution of the infills

to the total stiffness of the model is small compared to that of the shear-wall. Based on the above considerations, the same limit strain values were specified for both bare and infilled dual structures. The same procedure is followed for the definition of the limit state values for the steel structures, namely the warehouse and the crane.

The definition of limit states on the seismic capacity curves for the different RC building typologies and the steel structures considered can be found in details in the full STREST D4.1 (Salzano et al. 2015). Then the tsunami nonlinear static analyses are performed to verify (or potentially slightly modify) the selected limit state values. Detailed results of the Deliverable Report are not reported here for the sake of brevity.

It must be noted that the tsunami capacity curves are not extracted from a single nonlinear static analysis as for the seismic case but from the total number of the tsunami nonlinear static time history analyses. This is done considering that the location and amplitude of the applied tsunami forces changes as a function of the inundation depth. It is worth noticing however that the seismic and tsunami capacity curves present consistent results predicting very similar damage state limits.

The selected limit state values finally adopted for the tsunami vulnerability analysis are presented in Table 3.5 and Table 3.6 for the RC buildings and the steel structures respectively.

Table 3.5 Definition of limit states for the different RC building typologies considered

Limit states	Steel strain (ϵ_s)		
	MRF bare frames	MRF with infills	Dual with/without infills
Limit state 1	0.002 (Steel bar yielding)	0.0007 (infills cracking)	0.002 (Steel bar yielding)
Limit state 2	0.0125	0.002 (Steel bar yielding)	0.0125
Limit state 3	0.025	0.010	0.04
Limit state 4	0.045	0.020	0.08

Table 3.6 Definition of limit states for the warehouse and the crane

Limit states	Steel strain (ϵ_s)	
	Warehouse	Crane
Limit state 1	0.00112 (Steel bar yielding)	0.00125 (Steel bar yielding)
Limit state 2	0.0125	0.0125
Limit state 3	0.03	0.03
Limit state 4	0.055	0.055

3.3.2 Construction of fragility curves

Fragility curves describe the probability of exceeding predefined levels of damage under a tsunami event of a given intensity. The results of the nonlinear numerical analysis (inundation depth - steel strain values) are used to derive fragility curves expressed as two-parameter time-variant lognormal distribution functions.

The following equation gives the cumulative probability of exceeding a DS conditioned on a measure of the tsunami intensity IM :

$$P[DS_i | IM] = \Phi \left[\frac{\ln(IM) - \ln(\overline{IM}_i)}{\beta} \right] \quad (3.3)$$

where, Φ is the standard normal cumulative distribution function, IM is the intensity measure of the tsunami expressed in terms of inundation depth (in units of m), \overline{IM}_i and β are the median values (in units of m) and log-standard deviations respectively of the building fragilities for each damage state i and DS_i is the damage state. The median values of inundation depth respectively corresponding to the prescribed damage states are determined based on a regression analysis of the nonlinear static analysis results (inundation depth - steel strain pairs) for each structural model. More specifically, a second order polynomial fit of the logarithms of the inundation depth - steel strain data, which minimizes the regression residuals, is adopted in all cases. Fig. 3.11 shows indicatively the derived inundation depth - steel strain relationships for the MRF 2-storey infilled building.

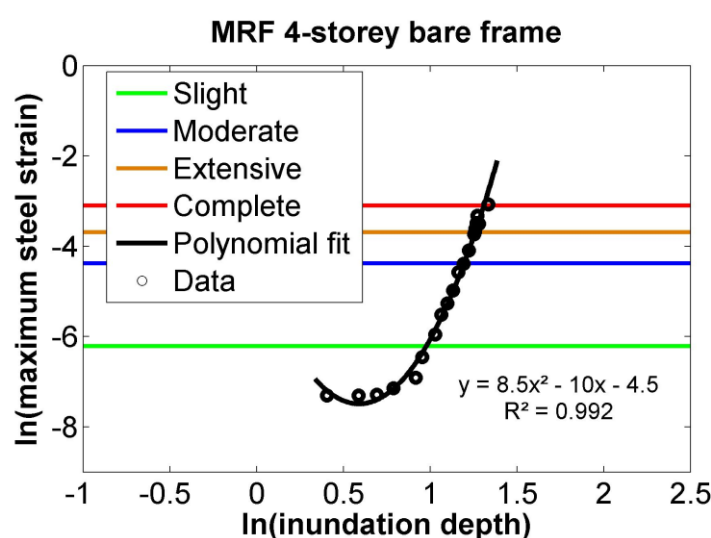


Fig. 3.11 Inundation depth- steel strain relationships for the MRF 2-storey infilled building

The various uncertainties are taken into account through the log-standard deviation parameter β , which describes the total dispersion related to each fragility curve. The primary sources of uncertainty which contribute to the total variability for any given damage state are those associated with the capacity of each structural type and the demand. The log-standard deviation value in the definition of the capacity is assumed to be equal to 0.3 for low code buildings (FEMA, 2004) and 0.25 for the modern jumbo crane. The uncertainty in the demand was considered by calculating the dispersion of the logarithms of inundation depth - steel strain simulated data with respect to the regression fit. Under the assumption that these two log-standard deviation components are statistically independent, the total log-standard deviation is estimated as the root of the sum of the squares of the component dispersions. The herein computed log-standard deviation β values of the curves vary from 0.33 to 0.59 for all structural models. Table 3.7 presents the lognormal distributed fragility parameters (median and log-standard deviation) in terms of inundation depth, and illustrates the corresponding sets of fragility curves for the various RC building typologies and for the warehouse and the crane respectively.

Table 3.7 Parameters of fragility functions

Structural system	Median inundation depth (m)				Dispersion β
	LS1 (m)	LS2 (m)	LS3 (m)	LS4 (m)	
MRF 2-storey bare-frames	1.85	2.38	2.56	2.71	0.43
MRF 2-storey infilled	1.16	1.57	2.11	2.33	0.37
Dual 2-storey bare-frames	1.14	1.57	1.83	1.99	0.40
Dual 2-storey infilled	0.96	1.27	1.46	1.57	0.44
MRF 4-storey bare-frames	2.66	3.30	3.52	3.70	0.33
MRF 4-storey infilled	1.81	2.43	3.33	3.74	0.40
MRF 9-storey bare-frames	4.01	4.97	5.30	5.57	0.39
MRF 9-storey infilled	2.27	3.81	5.49	6.19	0.35
Warehouse	2.20	2.79	2.97	3.10	0.57
Crane	13.14	15.37	16.16	16.69	0.59

It may be observed that, the higher the height of the RC building, the lower its vulnerability. It is also shown that the low-rise and mid-rise models with infills are more vulnerable compared with the corresponding models with bare frames. This trend also holds true for the high-rise MRF for the exceedance of slight and moderate damage. This is in accordance with the FEMA guideline, which recommends the design of vertical evacuation buildings with break-away walls or open construction in the lower levels to allow water to pass through with minimal resistance.

In contrast, when extensive or complete damage of the structures is anticipated, the bare RC frame is expected to sustain larger damages in comparison with the corresponding infilled one. This could be attributed to the height of the building, which makes its behaviour unpredictable for higher levels of damage.

Furthermore, it is seen that the low-rise dual RC models are more vulnerable compared to the corresponding MRFs. The latter could be related to the concentration of large tsunami forces in shear walls. This is the reason why FEMA recommends that for the design of vertical evacuation structures, shear walls should be oriented parallel to the anticipated direction of tsunami flow to reduce associated tsunami forces.

Regarding the steel structures, i.e. the warehouse and the crane, it is seen that although the numerically calculated limit state values are the same for all damage states, they present, as it would be expected, a completely different behavior in terms of fragility. In particular, the warehouse presents fragility values that are generally closer to that of the low-rise and mid-rise MRF RC buildings while the crane, as it would be expected, is significantly less vulnerable compared to all building types analyzed. It is also observed that the derived curves for the warehouse are very close together. Thus, once the warehouse has yielded, it will very rapidly also attain the post-yield limit states.

The representative comparisons of the herein developed numerical tsunami fragility curves with the corresponding empirical ones of Suppasri et al. (2011) (Indian Ocean tsunami in Thailand) and Suppasri et al. (2013) (Great East Japan tsunami) are represented in detail in STREST D4.1 (Salzano et al. 2015). However, a good agreement between the curves is observed in general. The existing differences can be attributed to the fact that the empirical fragility curves chosen for comparison were constructed based on hazard-damage relationships from previous different tsunami events (i.e. the Indian Ocean tsunami in Thailand and the Great East Japan tsunami) and/or expert judgment. In addition, the proposed fragility curves refer to low code buildings in contrast to the empirical ones that include different design codes. Therefore, only preliminary comparisons of the herein numerically developed fragility curves with the empirical ones can be made as the latter are highly specific to a particular seismo-tectonic, geotechnical and built environment.

4. Distributed critical infrastructures

The impact of several recent destructive events to critical infrastructures (CIs) highlighted the need to develop guidelines for the performance and consequences assessment of geographically distributed non-nuclear CIs exposed to multiple natural hazards and low probability-high consequence (LP-HC) events. To accomplish this, quantitative and standardized procedures and tools for consequence analysis of those CIs are presented. Some key components of this assessment are: the identification of hazards to which the CI components are exposed, the vulnerability models that evaluate the extent to which a particular component can withstand the impact of the hazard and the systemic analysis that measures the performance of the infrastructure under given hazards.

During the same event, different hazard intensities may be experienced at the different locations where components are located. Such intensities cannot be assumed independent, since they are caused by the same source event. Also, different components may be sensible to different intensity measures (IMs) related to the same hazard (e.g. for ground shaking, to PGA and PGV), or to secondary hazards (e.g. PGD for geotechnical hazards). Thus, it is necessary to model the potential spatial correlations of the hazard intensities as well as the spatial cross-correlation between different IMs. STREST ERR2 (Cotton et al. 2016) provides guidelines for harmonized hazard assessment for high-consequences events.

Fragility or vulnerability functions should be estimated both for single adverse events and for cascades of adverse events. While the evaluation of the seismic vulnerability has received over the past years a significant attention (e.g. Calvi et al. 2006; Pitilakis et al. 2014a), the vulnerability assessment of structures related to other hazards (e.g. tsunamis, floods, landslides etc.) is still limited (e.g. Karafagka et al. 2016; Fotopoulou and Pitilakis, 2013). Therefore, there is a need to expand the vulnerability and risk assessment methods developed for seismic hazard to other hazards. In the framework of STREST (Kakderi et al. 2015), a comprehensive review of fragility functions for the critical components of the selected geographically distributed CIs was carried out and new fragility curves were developed where necessary. It is noted that with the fragility functions only the potential physical damages of the components of the systems are considered (the functionality of either the elements or the whole system is not considered). The damage states (physical damage) of the components are usually correlated with functionality levels and restoration times. To assess the vulnerability and performance at system level, except for the previously described methods, different complementary approaches should be followed, i.e. a connectivity analysis, a capacity analysis or a fault-tree analysis (e.g. Pitilakis et al. 2014b).

Complex systems exhibit patterns, outcomes, and properties not present in any of their individual elements. In this case, the performance of the whole infrastructure (CI facility) should be based on integrated models and evaluation measures of critical infrastructure systems. The quantitative measure of the performance of a system and its elements when subjected to a hazard is given by Performance Indicators (PI's). They express numerically either the comparison of a demand with a capacity quantity, or the consequence of a mitigation action, or the assembled consequences of all damages (the "impact"). Performance indicators, at the component or the system level, depend on the type of analysis that is performed.

In the following, the description of the vulnerability and loss models developed for each of the three selected case studies of geographically distributed CIs, i.e. CI-B1: Major Hydrocarbon Pipelines in Turkey, CI-B2: Gasunie National Gas Storage and Distribution Network in Holland and CI-B3: Port Infrastructures of Thessaloniki in Greece are provided. It is noted that certain components of CI-B3 have already been addressed in section 3 as part of individual, single-site infrastructures.

4.1 CI-B1: Major Hydrocarbon Pipelines in Turkey

4.1.1 Vulnerability models

The major hydrocarbon pipelines in Turkey consist of continuous buried steel pipes with welded connections. Such high quality pipes are not much sensitive to wave propagation (WP) hazard since the induced strains due to wave propagation is very low as compared to the permanent ground deformation (PGD) hazard. The potential damages of pipelines can be assessed using fragility functions, which relate the pipeline damage rates to different level of seismic intensity. The damage rates of buried pipes are often defined as the number of pipe repairs (RR) per unit length of pipeline, while the seismic intensity is quantified via a series of ground motion parameters calculated with seismic records. The few available empirical fragility relations for welded-joint continuous steel pipelines are reviewed in Kakderi et al. (2015). In order to access the seismic performance of buried hydrocarbon pipelines due to fault offset, the existing fragility functions are not adequate. Therefore, new fragility relations are developed based on nonlinear numerical analysis of the pipe and the surrounding soil (Salzano et al. 2015).

4.1.2 Performance and loss assessment

A full probabilistic risk assessment of pipeline failure at fault crossings is developed for the performance and loss assessment of the CI-B1. The seismic risk of pipeline failure is expressed as the annual probability of pipeline failure at crossings. Through case studies, a set of key parameters has been investigated about the impact on the seismic risk of pipeline failure due to fault displacement. Two important aleatory uncertainties from earthquakes are considered during the risk analysis: fault displacement and fault-pipe crossing angle. The influence of these uncertainties on the risk of pipe failure at strike-slip fault crossings is studied. Uncertainty of pipeline parameters and soil, such as soil property, can also be taken into account in the pipeline failure risk. The seismic risk of pipeline failure due to the actual fault rupture occurring at a distance far away from the mapped fault trace is also examined. This quantitative risk can be used as a useful reference for engineers to design and retrofit pipes at fault crossings.

4.2 CI-B2: Gasunie National Gas Storage and Distribution Network in Holland

4.2.1 Vulnerability models

For the Gasunie gas pipelines, the specific mechanism of soil liquefaction and corresponding lateral displacements is investigated as it is identified as one of the main failure mechanisms for the pipelines. Taking into account the scarce available damage data for these conditions, numerical analyses were conducted to develop fragility functions (Miraglia et al. 2015). Regarding the Gasunie processing stations, some of them are open while others are housed in buildings. Most buildings are relatively new and regular, either masonry or concrete. Following Gehl et al. (2014), a fault-tree decomposition of the sub-components was used to assess the relative vulnerability of these stations.

4.2.2 Performance and loss assessment

For the CI-B2, dedicated performance indicators should express the character of supply and demand of gas delivery as well as the presence of redundancies. Hence, focus is

given on connectivity analysis and capacity analysis (apart from mere physical damages of the components of the systems) and appropriate performance indicators, such as Serviceability loss (SR) and Connectivity loss (CL), could be used. The backbone of the proposed performance and risk assessment is the methodology of SYNER-G (Pitilakis et al. 2014b). The methodology was also followed by Esposito et al., 2015 for the seismic risk analysis of gas distribution networks. It includes the “Shakefields” method (Weatherill et al. 2014) for maps of sampled correlated seismic intensities at the sites of the nodes and branches in the gas distribution network. The gas distribution network itself is modelled as a graph composed by the set of nodes connected by edge links amongst each other. The stations, regulators groups and joints are thus represented by nodes while pipes are represented by links. Through MC sampling of events, annual exceedance curves of the performance indicators are calculated, making use of fragility curves for pipelines and stations.

4.3 CI-B3: Port Infrastructures of Thessaloniki in Greece

4.3.1 Vulnerability models

Regarding the port infrastructures of Thessaloniki, existing seismic fragility functions for the most critical components to the functionality of the port, namely waterfront structures (e.g. NIBS 2004; Ichii 2003 and 2004; Kakderi and Pitilakis 2010; etc.) and cranes (e.g. NIBS 2004; Kosbab 2010), exposed to seismic hazards (ground shaking and liquefaction) were reviewed in Kakderi et al. (2015). Fragility functions for other components, e.g. building structures, liquid facilities etc., can be found in Pitilakis et al. (2014a). Finally, in the framework of STREST (Karafagka et al. 2016; Salzano et al. 2015) new analytical tsunami fragility curves for buildings of various typologies and container cranes infrastructures were constructed as part of the CI-B3 case study (see section 3.3).

4.3.2 Performance and loss assessment

For the assessment of complex system performance such as port facilities, contributions of all components, and their interactions, have to be appropriately accounted for. For the case of the CI-B3, a specific methodology and tools are proposed for the assessment of the systemic performance and loss of harbours, simulating port operations and considering also the interactions among the main port elements. Performance and loss assessments are based on the general framework of SYNER-G. This methodology potentially accounts also for epistemic uncertainty, taking into consideration uncertainty in models’ parameters (through a hierarchical acyclical chain of probabilistic distributions). In addition, it can be applied within techniques like Logic Trees or Ensemble Modelling (see D3.1, Selva et al. 2015) to quantify also epistemic uncertainty. The methodology has been originally designed for seismic hazard (Cavaliere et al. 2012; Argyroudis et al. 2015), and was extended for tsunami hazard (Pitilakis et al. 2016). The functionality of the harbour is assessed through system-level Performance Indicators (PIs), which are related to the containers and cargo traffic. The analysis is based on an object-oriented paradigm where systems are described through a set of classes, characterized in terms of attributes and methods, interacting with each other. The objective of the analysis was to evaluate probabilities or mean annual frequency of events defined in terms of loss in performance of networks.

5. Multiple-site, low-risk, high-impact, non-nuclear critical infrastructures

STREST Deliverable 4.3 (2015) provides a framework for the performance and consequences assessment of multiple-site, low-risk high-impact non-nuclear critical infrastructures subjected to strong ground shaking during earthquakes. Industrial districts have been selected as an example of this type of non-nuclear critical infrastructure for the purposes of the aforementioned guidelines. Precast concrete warehouses that are typically found in industrial districts in Europe, and that have demonstrated high levels of damage in past earthquakes (described further in STREST Deliverable 2.3, 2014) have been used as an application of the guidelines. Damage to these buildings can affect the structural system, the non-structural components (such as the external cladding), and the contents of the building, thus leading to a number of direct economic losses and the time required to repair the damage leads to additional business interruption losses, all of which are covered in the guidelines.

5.1 CI-C1: Industrial district, Italy

5.1.1 Structural and non-structural fragility

Building typologies

Three different classes of typical European precast warehouse buildings, which represent the majority of precast buildings in the Tuscany region, have been considered in the guidelines.

Buildings in all the considered building classes consist of parallel portals composed of beams placed on corbel connections at the top of the columns. A neoprene pad is usually inserted between the elements and, depending on the building class, additional dowels are provided. Columns are fixed at the bottom by socket foundations. Parallel portals support a roof system, which is an assembly of precast elements (girders, TT slabs, hollow core slabs), and, in the case of a seismic event, does not behave as a rigid diaphragm (Magliulo et al. (2014), Liberatore et al. (2013), Casotto et al. (2015) and Belleri et al. (2014)).

Within the considered building classes there are two types of structural configuration: type 1 (building class 1) and type 2 (building classes 2 and 3). Buildings with type 1 structural configuration (Fig. 5.1a) contain long saddle roof beams, whereas type 2 structural configuration (Fig. 5.2b) is distinctive of buildings with shorter rectangular beams and larger distance between the portals. Depending on the time of construction, the code level of a building class is either pre-code (building classes 1 and 2) or low-code (building class 3) for buildings built before or after 1996, respectively. Pre-code buildings were designed to withstand lateral load equal to 2 percent of the building self-weight, whilst design lateral load of low-code buildings amounted to 7 percent of the building self-weight. Moreover, due to different requirements in the design regulations it was assumed that beam-to-column connections in the pre-code buildings depended only on friction, whereas additional dowels were assumed to be implemented in the beam-to-column connections of the low-code buildings. For more information about the building classes, the reader is referred to Casotto et al. (2015) and STREST Deliverable 4.3 (2015).



Fig. 5.1 Structural configuration of Italian precast warehouses

Furthermore, the most common types of claddings in precast buildings in the Tuscany region (Regione Toscana direzione generale politiche territoriali n.d.), i.e. vertical precast panels, horizontal precast panels and concrete masonry infills, were considered. In combination with the three building classes, these non-structural components defined eight subclasses.

Vertical and horizontal panels are stiff elements, attached, respectively, to the beams and columns (Isaković et al., 2012). Their seismic performance is mainly dependent on the fastenings, which are provided at the top of the panels in order to prevent the panels from overturning. Fastenings may fail due to large relative displacements between the panels and the structure or due to inertial forces perpendicular to the plane of the panels.

Concrete masonry infills are usually situated between columns (Regione Toscana direzione generale politiche territoriali n.d.). Due to a poor connection with the adjacent beam, negligible vertical load is transmitted from the roof, which can lead to the infills overturning. Such failures were observed after recent Italian earthquakes (Belleri et al., 2014). For more information about the considered non-structural components the reader is referred to Babič and Dolšek (2016) and STREST Deliverable 4.3 (2015).

Numerical models

Numerical models of precast buildings have been developed in the OpenSees finite elements platform (McKenna and Fenves, 2010). The models consist of portals, connected by the roof system. Different non-structural elements can be attached to the portals using springs, which are added to the model in the form of one-dimensional and zero-length elements.

Each portal is composed of columns and beams. Columns are modelled by one component lumped plasticity elements. Beams are modelled as elastic elements connected to the columns by the contact zero-length elements based on Mohr-Coulomb frictional law, thus allowing the beams to slip from the columns, while considering interaction between accelerations in vertical and horizontal directions. In addition to the contact element, an elastic no-tension spring with an initial gap is modelled between a column and a beam to emulate the possible impact between the two elements. In the case of low-code structures, dowels are modelled in each beam-to-column connection with an additional shear spring, which is removed from the model during the analysis, if the strength of the dowels is attained. The roof system is modelled by truss elements, resulting in a flexible performance.

In the in-plane direction (parallel to the plane of the panels) vertical panels are modelled as non-linear springs connecting beams to fixed nodes. In the out-of-plane direction (perpendicular to the plane of the panels) vertical panels can be modelled independently as nodal masses connected to the beams by linear springs.

Horizontal panels can be modelled by elastic elements with high stiffness, which are attached to the columns (Fig. 5.2). The mass can be lumped at the centre of each panel. The vertical connections at the bottom (corbels) can be modelled as contact zero-length elements based on Mohr-Coulomb frictional law. Sliding of the panels is allowed in the in-plane direction, whereas displacements in the out-of-plane direction are prevented by an additional elastic spring. Moreover, the in-plane drifts are limited at the end of the gap provided for the panel installation by an additional elastic no-tension spring. At the top of each panel, panel-to-structure connections (either sliding or pinned) in the in-plane direction can be modelled by non-linear springs. In the out-of-plane direction fastenings are modelled by an elastic spring with high stiffness, which prevents displacements.

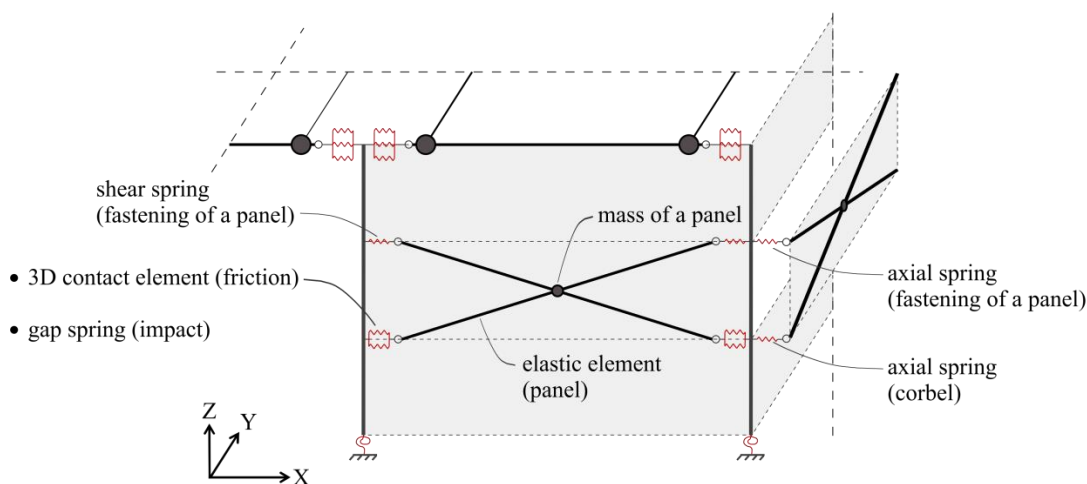


Fig. 5.2 A schematic illustration of numerical model of a building with horizontal panels

Masonry infills can be modelled by stiff elastic elements and zero-length elements. The mass may be lumped at the centre of the infill. The infill-to-foundation connection can be modelled by two elastic no-tension springs, thus allowing rocking of the infill in the out-of-plane direction. Connections to the adjacent columns are modelled by the impact zero-length elements, which are able to capture frictional effects in the out-of-plane direction and impact in the in-plane direction. Note that in buildings with masonry infills, an additional plastic hinge is placed at the infill-column joint at the top of the infill to capture the non-linear behaviour of the column.

For more information about the numerical models the reader is referred to Babič and Dolšek (2016) and STREST Deliverable 4.3 (2015).

5.1.2 Contents fragility

The most commonly damaged contents in industrial buildings have been found by Porter et al. (2012) to be:

- Fragile stock and supplies on shelves
- Computer equipment
- Industrial racks
- Movable manufacturing equipment.

A simplification of the procedure in ATC-58 (ATC, 2012) as proposed by Porter et al. (2012) is recommended in the guidelines for large industrial districts. The ATC-58 damage-analysis procedure provides component damage in discrete damage states using fragility functions derived from experiments, earthquake experience, first

principles and, in some cases, expert judgment. Porter et al. (2012) have taken the fragility functions from ATC-58 that most closely fit the contents typologies described above, leading to proposed lognormal distribution parameters. In some cases the restraint of the contents (poor, moderate or superior) can also be accounted for. The intensity measure type in all cases is peak floor acceleration (in g), which in the case of single storey industrial buildings can be taken as the peak ground acceleration.

5.1.3 Vulnerability models

Once fragility functions for structural/non-structural components and contents have been developed, the next stage is to transform these into vulnerability functions, which describe the probability of loss conditioned on a level of ground shaking. This is done through damage-loss models.

The damage-loss models for structural and non-structural components are defined by damage factors corresponding to designated damage states. Damage factors for structural components refer to the portion of construction cost of the bearing structure (without non-structural components) that is required to repair the damage state. These damage factors also account for additional costs due to demolition and removal of debris, where necessary. Damage factors for non-structural components refer to the portion of construction cost of the non-structural components required to repair the damage.

For contents, there is only one damage state for each component and the consequence of damage is that the component must be replaced, hence the mean damage factor is 100%. If the structure collapses, then the damage factor for contents is assumed to be 100%.

Business interruption (or downtime) is defined as the time needed to repair building damage, and has been divided into the following two components, following the recommendations of Mitrani-Reiser (2008) and Terzic et al. (2015):

- Mobilisation time (i.e. the time to undertake damage assessment, consultations with professional engineers, the contractor bidding process, debris clean-up, financing, contractor mobilisation etc. that needs to be completed before repairs can begin).
- Repair time (i.e. the time to return the structure to its pre-earthquake condition).

The financial loss due to this time may arise due to the loss in income from renting the damaged facility or the loss of daily revenue of the business. Additionally, in the case that the owner of a business is located in the facility, additional losses due to relocation cost and renting of new facilities may need to be considered. The potential sources of loss will need to be assessed on a case-by-case basis and used to define the business interruption value in the exposure model.

For each damage states defined for the structural and non-structural damage, it is expected that building and business owners will consult with local contractors to estimate the mobilisation and repair time. Given that these are uncertain quantities, both the mean and dispersion values will need to be estimated, based on empirical data, literature review of past case studies and expert judgement.

5.2 Probabilistic multi-site loss modelling

The output of a probabilistic multi-site loss assessment is a loss exceedance curve. Once stochastic event sets and associated ground-motion fields (for each event) have been computed, the intensity measure level at a given site in the exposure model is used to extract the loss ratio from each vulnerability function that has been defined for the industrial facility at that site. The loss ratios that are sampled for assets of a given

taxonomy industrial facility category at different sites can be considered to be either independent or fully correlated. The latter case might be chosen, for example, when all facilities have been constructed by the same contractor. The losses for a given industrial facility are calculated using all of the ground-motion fields, leading to list of events and associated structural/non-structural/contents loss ratios and downtime. The loss ratios and downtime are multiplied by the value of each specified in the exposure model and summed to give a total loss for the facility. For a given industrial facility, this list is then sorted from the highest loss to the lowest. The rate of exceedance of each loss is calculated by dividing the number of exceedances of that loss by the total length of the stochastic event sets (in years). In the case where aftershocks are not included in the event sets, it is possible to assume a Poissonian distribution of the earthquake occurrence model and calculate the probability of exceedance of each loss accordingly.

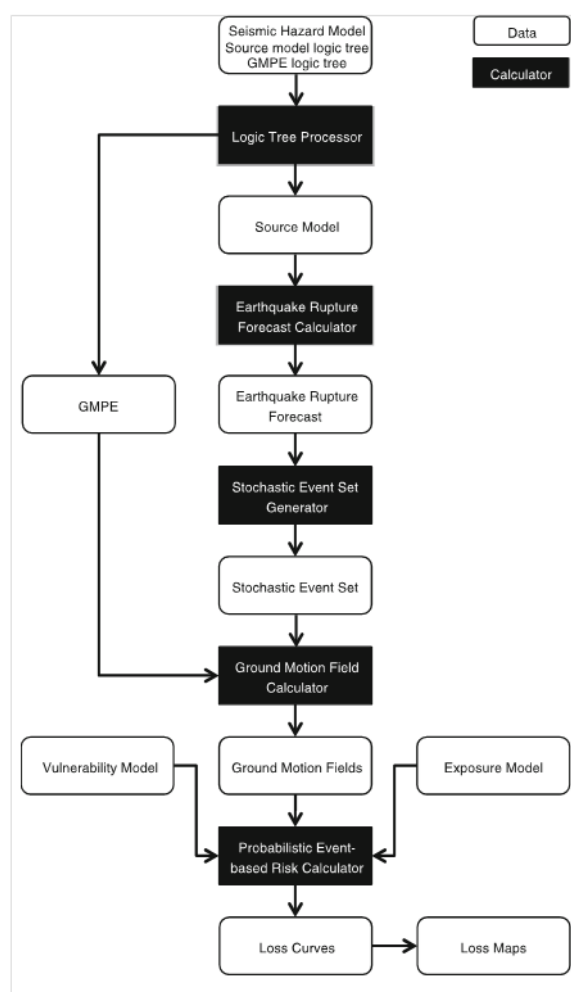


Fig. 5.3 A schematic illustration of numerical model of a building with horizontal panels

If an aggregate loss curve for the whole portfolio of industrial facility is required, it is necessary to sum the losses from all the industrial facility in the exposure file, per event, before calculating the exceedance frequency of loss. All of these calculations can be done with the OpenQuake-engine, as described further in Silva et al. (2013) and Crowley and Silva (2013).

6. Conclusions

This reference report addressed guidelines for vulnerability assessment of critical infrastructures exposed to natural hazards. The work of WP4 started from the fact that vulnerability assessment of critical infrastructures to natural hazards, differently to ordinary structures, has to primarily target the cascading effects the natural event may induce, as they are generally the main loss drivers. Although the interested reader is referred to the WP4 deliverables for further insights, the main conclusions from the discussed efforts may be listed as follows:

1. A common approach to taxonomy, which is the basic component of vulnerability assessment, may be addressed for all typologies of CIs considered;
2. In more general terms, it appears that a common probabilistic framework may be applied independently of the specific features of the considered infrastructure and may be applied also to systems of interdependent infrastructures;
3. However, the models needed to put this vulnerability assessment in practice are mostly lacking, this applies especially for natural hazard different for the seismic one (although also the seismic case is far to be complete for many situations);
4. For the same reason as #3, also models to consider multi-event and/or multi-hazard loss assessment is far to be addressed, although the track on which such a research should develop appears clear at this point.

References

1. API 620 (2015). Design and Construction of Large Welded Low Pressure Storage Tanks. Washington D.C., USA: American Petroleum Institute.
2. API 650 (2015). Welded Steel Tanks for Oil Storage. Washington D.C., USA: American Petroleum Institute
3. Applied Technology Council (ATC) (2012). ATC-58: Guidelines for Seismic Performance Assessment of Buildings, 100% Draft. Redwood City, CA.
4. Argyroudis, S., Selva, J., Gehl, P., Pitilakis, K. (2015). Systemic Seismic Risk Assessment of Road Networks Considering Interactions with the Built Environment. *Computer-Aided Civil and Infrastructure Engineering* 30: 524–540
5. Babič, A., Dolšek, M. (2016). Seismic fragility functions of industrial precast building classes. *Engineering Structures* (in press).
6. Baker, J.W., Cornell, C.A. (2006). Correlation of response spectral values for multicomponents of ground motion. *Bulletin of the Seismological Society of America* 96(1): 215–227
7. Belleri, A., Brunesi, E., Nascimbene, R., Pagani, M., Riva, P. (2014). Seismic performance of precast industrial facilities following major earthquakes in the Italian territory. *Journal of Performance of Constructed Facilities*, 29(5), 04014135.
8. Bird, J.F., Crowley, H., Pinho, R. & Bommer, J.J. (2005). Assessment of building response to liquefaction induced differential ground deformation". *Bul. of the New Zealand Society for Earthquake Engineering* 38(4), 215-234.
9. Calvi, G.M., Pinho R., Magenes, G., Bommer, J.J., Restrepo-Velez, L.F. & Crowley H. (2006). Development of seismic vulnerability assessment methodologies over the past 30 years. *J Earthq Technol* 43(3): 75–104
10. Campedel, M., Cozzani, V., Garcia-Agreda, A., & Salzano, E. (2008). Extending the Quantitative Assessment of Industrial Risks to Earthquake Effects. *Risk Analysis* 5, 1231-1246.
11. Casotto, C., Silva, V., Crowley, H., Nascimbene, R., & Pinho, R. (2015). Seismic fragility of Italian RC precast industrial structures. *Engineering Structures*, 94, 122-136.
12. Cavalieri, F., Franchin, P., Gehl, P. & Khazai, B. (2012). Quantitative assessment of social losses based on physical damage and interaction with infrastructural systems. *Earthquake Engineering and Structural Dynamics* 41(11):1569–89
13. Chen, Q., Seifried, A., Andrade, J.E. & Baker, J.W. (2012). Characterization of random fields and their impact on the mechanics of geosystems at multiple scales. *International Journal for Numerical and Analytical Methods in Geomechanics* 36(2):140–165
14. Cotton F et al. (2016). Reference report 2: Guidelines for harmonized hazard assessment for high-consequences events, covered in STREST, STREST project: Harmonized approach to stress tests for critical infrastructures against natural hazards
15. Crowley, H. & Bommer, J.J. (2006). Modelling seismic hazard in earthquake loss models with spatially distributed exposure, *Bulletin of Earthquake Engineering*, 4(3), 249-273
Crowley, H., Pinho, R., & Bommer, J. (2004). A probabilistic displacement-based vulnerability assessment procedure for earthquake loss estimation. *Bull Earthq Eng.* 2, 173–219.

16. Crowley, H., Silva, V. (2013). *OpenQuake Engine Book: Risk v1.0.0*. GEM Foundation, Pavia, Italy.
17. de Moel, H., & Aerts, J.C.J H. (2011). Effect of Uncertainty in Land Use, Damage Models and Inundation Depth on Flood Damage Estimates. *Natural Hazards* 58, 407–25.
18. Esposito, S., Iervolino, I., d'Onofrio, A., Santo, A., Cavalieri, F. & Franchin, P. (2015) Simulation-Based Seismic Risk Assessment of Gas Distribution Networks. *Computer-Aided Civil and Infrastructure Engineering* 30(7): 508–523.
19. Esposito, S., Iervolino, I. (2011). PGA and PGV spatial correlation models based on European multievent datasets. *Bulletin of the Seismological Society of America* 101(5):2532–2541
20. Esposito, S., Iervolino, I. (2012). Spatial correlation of spectral acceleration in European data. *Bulletin of the Seismological Society of America* 102(6): 2781–2788
21. FEMA. (2004). *Direct physical damage—general building stock*. HAZUS-MH Technical manual, Chapter 5. Washington, D.C: Federal Emergency Management Agency.
22. Fotopoulou, S, & Pitilakis, K. (2013). Vulnerability assessment of reinforced concrete buildings subjected to seismically triggered slow-moving earth slides. *Landslides* 10:563–582. doi: 10.1007/ s10346-012-0345-5
23. Fotopoulou, S., & Pitilakis, K. (2013a). Fragility curves for reinforced concrete buildings to seismically triggered slow-moving slides. *Soil Dynamics and Earthquake Engineering* 48, 143–161.
24. Fotopoulou, S., & Pitilakis, K. (2013b). Vulnerability assessment of reinforced concrete buildings subjected to seismically triggered slow-moving earth slides. *Landslides* 10, 563-582.
25. Galbusera, L., Azzini, I., & Giannopoulos, G. (2015a). A Methodology for Resilience Optimisation of Interdependent Critical Infrastructures. In *Critical Information Infrastructures Security* (pp. 56-66). Springer International Publishing. In *A Methodology for Resilience Optimisation of Interdependent Critical Infrastructures*. In *Critical Information Infrastructures Security* (pp. 56-66). Springer International Publishing
26. Galbusera, L., Azzini, I. & Giannopoulos, G. (2015b). Assessing the recovery resilience of the port of Thessaloniki using GRRASP. *Ispra (Italy): JRC Technical Reports JRC94541*, European Commission.
27. Galbusera, L., Ntalampiras, S., Azzini, I. & Giannopoulos, G. (2013). Resilience assessment and optimization methodology for critical infrastructures. *Ispra (Italy): JRC Technical Reports JRC85475*, European Commission
28. Gehl, P., Desramaut, N., Arnaud Réveillère, A., Modaressi, H. (2014) Fragility Functions of Gas and Oil Networks. In K. Pitilakis et al. (eds.), *SYNER-G: Typology Definition and Fragility Functions for Physical Elements at Seismic Risk, Geotechnical, Geological and Earthquake Engineering* 27, DOI 10.1007/978-94-007-7872-6_7, Springer , Netherlands, pp. 197-218
29. Goda, K., Atkinson, G.M. (2009). Probabilistic characterisation of spatial correlated response spectra for earthquakes in Japan. *Bulletin of Seismological Society of America* 99(5): 3003–3020
30. Goda, K., Hong, H.P. (2008). Spatial correlation of peak ground motions and response spectra. *Bulletin of Seismological Society of America* 98(1): 354–365
31. Hancilar, U. & Taucer, F. (Ed.) (2013) *Guidelines for typology definition of European physical assets for earthquake risk assessment*, SYNER-G Reference

- Report 2, Available from URL: http://www.vce.at/SYNER-G/pdf/reference_reports/RR2-LB-NA-25883-EN-N.pdf
32. HAZUS-MH MR4. (2009). The Federal Emergency Management Agency's (FEMA's) Methodology for Estimating Potential Losses from Disasters. National Institute of Building Science, Risk Management Solutions. Menlo Park, CA: Federal Emergency Management Agency.
 33. Ichii K (2003) Application of performance-based seismic design concept for caisson-type quay walls. Ph.D. dissertation, Kyoto University
 34. Ichii K (2004) Fragility curves for gravity-type quay walls based on effective stress analyses. In 13th WCEE, Vancouver, BC
 35. Iervolino, I., Giorgio, M., Galasso, C. & Manfredi, G. (2010). Conditional hazard maps for secondary intensity measures. *Bulletin of the Seismological Society of America* 100(6): 3312–3319
 36. Isaković, T. et al. (2012). Improved fastening systems of cladding wall panels of precast buildings in seismic zones, Ljubljana: University of Ljubljana
 37. Jayaram, N., Baker, J.W. (2009). Correlation model of spatially distributed ground motion intensities. *Earthquake Engineering and Structural Dynamics* 38:1687–1708
 38. Kakderi, K. et al. (2015). Deliverable 4.2: Guidelines for performance and consequences assessment of geographically distributed, non-nuclear critical infrastructures exposed to multiple natural hazards. STREST project EC/FP7 (2007-2013), grant agreement No: 603389
 39. Kakderi, K. & Pitilakis, K. (2010). Seismic analysis and fragility curves of gravity waterfront structures. In 5th international conference on recent advances in geotechnical earthquake engineering and soil dynamics and symposium in Honour of Prof. I. M. Idriss, Paper 6.04a
 40. Karafagka, S., Fotopoulou, S., Pitilakis, K. (2016). Tsunami fragility curves for seaport structures, 1st International Conference on Natural Hazards & Infrastructure, 28-30 June 2016, Chania, Greece
 41. Kosbab, B.D. (2010). Seismic performance evaluation of port container cranes allowed to uplift. PhD thesis, School of Civil and Environmental Engineering, Georgia Institute of Technology
 42. Krausmann, E., Cozzani, V., Salzano, E., & Renni, E. (2011). Industrial accidents triggered by natural hazards: an emerging risk issue. *Natural Hazards and Earth System Sciences*. 11, 921–929.
 43. Kreibich, H., Piroth, K., Seifert, I., Maiwald, H., Kunert, U., Schwarz, J., Merz, B., & Thieken, A.H. (2009). Is Flow Velocity a Significant Parameter in Flood Damage Modelling?. *Nat. Hazards Earth Syst. Sci.* 9, 1679-1692
 44. Liberatore, L. et al. (2013). Failure of industrial structures induced by the Emilia (Italy) 2012 earthquakes. *Engineering Failure Analysis*, 34, pp.629–647. Available at: <http://dx.doi.org/10.1016/j.engfailanal.2013.02.009>.
 45. Loth, C., Baker, J.W. (2013). A spatial cross-correlation model of spectral accelerations at multiple periods. *Earthquake Engineering and Structural Dynamics* 42:397–417
 46. Macabuag, J., Lloyd, T., & Rossetto, T. (2014). Towards the development of a method for generating tsunami fragility functions. *Proceedings of 2nd European Conference on Earthquake Engineering and Seismology*. Istanbul.
 47. Magliulo, G., Ercolino, M., Petrone, C., Coppola, O., & Manfredi, G. (2014). The Emilia earthquake: seismic performance of precast reinforced concrete buildings. *Earthquake Spectra*, 30(2), 891-912

48. Marzocchi, W., Taroni, M. & Selva, J. (2015). Accounting for Epistemic Uncertainty in PSHA: Logic Tree and ensemble Modeling. *Bull. Seism. Soc. Am.* 105(4):2151–2159, doi: 10.1785/0120140131
49. Matos, J.P., Mignan, A. & Schleiss A.J. (2015). Vulnerability of Large Dams Considering Hazard Interactions: Conceptual Application of the Generic Multi-Risk Framework. In 13th ICOLD International Benchmark Workshop on Numerical Analysis of Dams. Lausanne, Switzerland.
50. McKenna, F., Fenves, G.L. (2010). Open System for Earthquake Engineering Simulation (OpenSees). Available at: <http://opensees.berkeley.edu>.
51. Miraglia, S., Courage, W., Meijers, P. (2015). Fragility functions for pipeline in liquefiable sand: a case study on the Groningen gas-network. In Haukaas, T. (Ed.) Proceedings of the 12th International Conference on Applications of Statistics and Probability in Civil Engineering (ICASP12), Vancouver, Canada, July 12-15
52. Mitrani-Reiser, J. (2008). Risk management products team downtime model, primary resource document for the FEMA P-58 Seismic Performance Assessment of Buildings, Methodology and Implementation series of products (see ATC, 2012)
53. Musson, R.M.W. (1999). Probabilistic seismic hazard maps for the Balkan region, *Annali di Geofisc.* 42, no. 6, 1109–1124.
54. National Institute of Building Sciences (NIBS) (2004). HAZUS-MH: user's manual and technical manuals. Report prepared for the federal emergency management agency. National Institute of Building Sciences, Washington, DC
55. Oliver, D.S. (2003). Gaussian cosimulation: modelling of the cross-covariance. *Math Geol* 35(6): 681–698
56. Pagani, M., Monelli, D., Weatherill, G., Danciu, L., Crowley, H., Silva, V., Henshaw, P., Butler, L., Nastasi, M., Panzeri, L., Simionato, M. & Vigano, D. (2014). OpenQuake Engine: An open hazard (and risk) software for the Global Earthquake Model, *Seismological Research Letters*, Vol. 85, No. 3, pp 692-702
57. Park, J., Bazzurro, P., Baker, J.W. (2007). Modeling spatial correlation of ground motion intensity measures for regional seismic hazard and portfolio loss estimation. In: Kanada, Takada, Furuta (eds) Applications of statistics and probability in civil engineering. Taylor and Francis Group, London
58. Petersen, M.D., Dawson, T.E., Chen, R., Cao, T., Wills, C.J., Schwartz, D.P. & Frankel, A.D. (2011). Fault displacement hazard for strike-slip faults. *Bulletin of the Seismological Society of America* 101(2): 805–825
59. Pitilakis, K., Argyroudis, S., Fotopoulou, S., Karafagka, S., Kakderi, K. & Selva, J. (2016). Risk assessment of critical facilities to moderate and extreme seismic events including tsunamis. The case of the harbor of Thessaloniki, 1st International Conference on Natural Hazards & Infrastructure, 28-30 June 2016, Chania, Greece
60. Pitilakis, K., Crowley, H. & Kaynia, A. (Eds) (2014a). SYNER-G: Typology definition and fragility functions for physical elements at seismic risk. Buildings, lifelines, transportation networks and critical facilities. Series title: Geotechnical, Geological and Earthquake Engineering, 27, Springer, Netherlands
61. Pitilakis, K., Franchin, P., Khazai, B. & Wenzel, H. (Eds) (2014b). SYNER-G: Systemic seismic vulnerability and risk assessment of complex urban, utility, lifeline systems and critical facilities. Methodology and applications. Series: Geotechnical, Geological and Earthquake Engineering, 31, Springer, Netherlands
62. Pohl, R. (2000). Failure Frequency of Gates and Valves at Dams and Weirs. *International Journal on Hydropower & Dams.* 6, 77–81.
63. Porter, K., Cho, I. & Farokhnia, K. (2012). Contents seismic vulnerability estimation guidelines, Available from URL:

- <http://www.nexus.globalquakemodel.org/gem-vulnerability/posts/draft-content-vulnerability-guidelines>
64. Regione Toscana direzione generale politiche territoriali, Il rischio sismico nelle aree produttive. , p.32. Available at: http://www.rete.toscana.it/sett/pta/sismica/01informazione/banchedati/edilizia_privata/img_ediliziaprivata/report_capannoni.pdf [Accessed February 2, 2015].
 65. Salzano et al. (2015). Deliverable D4.1: Guidelines for performance and consequences assessment of single-site, high-risk, non-nuclear critical infrastructures exposed to multiple natural hazards, covered in STREST (AUTH contribution), STREST project: Harmonized approach to stress tests for critical infrastructures against natural hazards
 66. Salzano, E., & Cozzani, V. (2007). Quantitative Risk Assessment of Industrial Processes: The Path Towards a Global Approach. In L. G. Mason (Ed.), Focus on Hazardous Materials Research (pp. 25-47). New York: Nova Science Publishers.
 67. Salzano, E., Garcia-Agreda, A., Di Carluccio, A., & Fabbrocino, G. (2009). Risk assessment and early warning systems for industrial facilities in seismic zones. Reliab. Eng. Syst. Saf. 94, 1577-1584.
 68. Salzano, E., Iervolino, I., & Fabbrocino, G. (2003). Seismic risk of atmospheric storage tanks in the framework of Quantitative Risk Analysis. Journal of Loss Prevention in the Process Industry. 16, 403-409.
 69. Selva, J., Argyroudis, S. & Pitilakis, K. (2013). Impact on loss/risk assessments of inter-model variability in vulnerability analysis. Nat. Hazards 67:723–746
 70. Selva, J., Sarfraz, M.I., Taroni, M., Marzocchi, W., Cotton, F., Courage, W., Abspoel-Bukman, L., Miraglia, S., Mignan, A., Pitilakis, K., Argyroudis, S., Kakderi, K., Pitilakis, D., Tsinidis, G. & Smerzini, C. (2015). D3.1 – Report on the effects of epistemic uncertainties on the definition of LP-HC events. STREST project: Harmonized approach to stress tests for critical infrastructures against natural hazards.
 71. Silva, V., Crowley, H., Pagani, M., Monelli, D., Pinho, R. (2013). Development of the OpenQuake engine, the Global Earthquake Model's open-source software for seismic risk assessment. Natural Hazards, DOI: 10.1007/s11069-013-0618-x
 72. Smerzini, C., Pitilakis, K., Hasmemi, K., submitted (2016) Evaluation of earthquake ground motion and site effects in the Thessaloniki urban area by 3D finite-fault numerical simulations, Bulletin of Earthquake Engineering
 73. SSHAC, Senior Seismic Hazard Analysis Committee (2013). Practical Implementation Guidelines for SSHAC Level 3 and 4 Hazard Studies. U.S. Nuclear Regulatory Commission; NUREG-2117, Revision 1
 74. Stojadinovic, B. et al. (2016). Reference report: Guidelines for stress-test design for non-nuclear critical infrastructures and systems: Methodology. STREST project: Harmonized approach to stress tests for critical infrastructures against natural hazards
 75. STREST Deliverable 2.3, 2014. Deliverable 2.3: Report on lessons learned from recent catastrophic events" www.strest-eu.org
 76. STREST Deliverable 4.3, 2015. Deliverable 4.3: Guidelines for performance and consequences assessment of multiple-site, low-risk, high-impact, non-nuclear critical infrastructures (exposed to multiple natural hazards, etc.). www.strest-eu.org
 77. STREST Deliverable 4.4, 2015. Report on the taxonomy of CIs based on their vulnerability characteristics and exposure to natural hazard initiating events. www.strest-eu.org

78. Suppasri, A., Koshimura, S., & Imamura, F. (2011). Developing tsunami fragility curves based on the satellite remote sensing and the numerical modeling of the 2004 Indian Ocean tsunami in Thailand. *Natural Hazards Earth System Science*. 11, 173-189.
79. Suppasri, A., Mas E., Charvet I., Gunasekera, R., Imai, K., Fukutani, Y., Abe, Y., & Imamura, F. (2013). Building Damage Characteristics Based on Surveyed Data and Fragility Curves of the 2011 Great East Japan Tsunami. *Natural Hazards*. 66, 319-41.
80. Terzic, V., Mahin, S.A., Comerio, M.C. (2015). Using PBEE in seismic design to improve performance of moment resisting frames by base-isolation, *Earthquake Spectra*, under review
81. Tinti, S., Tonini, R., Bressan, L., Armigliato, A., Gardi, A., Guillande, R., Valencia, N., & Scheer S., (2011). *Handbook of Tsunami Hazard and Damage Scenarios*. Luxembourg.
82. Vugrin, E.D., Warren, D.E., Ehlen, M.A. & Camphouse, R.C. (2010). A framework for assessing the resilience of infrastructure and economic systems. In e. K. Gopalakrishnan and S. Peeta, *Sustainable and resilient critical infrastructure systems: simulation, modeling, and intelligent engineering* (pp. 77-116). Berlin: Springer-Verlag, Inc.
83. Wang, M., Takada T. (2005). Macrospatial correlation model of seismic ground motions. *Earthquake Spectra* 21(4):1137-1156
84. Weatherill, G., Esposito, S., Iervolino, I., Franchin, P. & Cavalieri, F. (2014). Framework for seismic hazard analysis of spatially distributed systems, in: K. Pitilakis et al. (eds). *SYNER-G: Systemic seismic vulnerability and risk assessment of complex urban, utility, lifeline systems and critical facilities. Methodology and applications*. Springer, Netherlands, 57-88
85. Weatherill, G., Silva, V., Crowley, H. & Bazzurro, P. (2015). Exploring the impact of spatial correlations and uncertainties for portfolio analysis in probabilistic seismic loss estimation, *Bulletin of Earthquake Engineering*, DOI 10.1007/s10518-015-9730-5
86. Woessner, J., Danciu, L., Giardini, D., Crowley, H., Cotton, F., Grunthal, G., Valensise, G., Arvidsson, R., Basili, R., Demircioglu, M., Hiemar, S., Meletti, C., Musson, R., Rovida, A., Sesetyan, K. & Stucchi, M. (2015). The 2013 European Seismic Hazard Model - Key Components and Results, *Bulletin of Earthquake Engineering*, DOI 10.1007/s10518-015-9795-1

List of abbreviations and definitions

CIs	Critical Infrastructures
CL	Connectivity loss
GMIMs	Ground Motion Intensity Measures
GMPEs	Ground Motion Prediction Equations
IMs	Intensity Measures
MC	Monte Carlo
MSRFs	Multi-Scale Random Fields
PGD	Permanent Ground Deformation
PIs	Performance Indicators
PSHA	Probabilistic Seismic Hazard Analysis
RR	The number of pipe repairs per unit length of pipeline
SR	Serviceability loss
ST	Stress Test
STREST	harmonized approach to stress tests for critical infrastructures against natural hazards

List of figures

Fig. 3.1 The process flow for the vulnerability function developed in D4.1 for the single-site industrial equipment.....	7
Fig. 3.2 Proposed framing of vulnerability and loss assessment for large dams. The analysis of potentially affected areas is downstream adds to the simulation of the dam system. The relationship between both “blocks” is achieved through flood wave routing.	13
Fig. 3-3 Vulnerability curve of the dam and foundation (left) and of the spillway element (right) to earthquakes	15
Fig. 3.4 Vulnerability of the bottom outlet element (left) and of the hydropower system (right) to earthquakes	15
Fig. 3.5 Distribution of the damage induced to the bottom outlet element by equipment malfunction (left) and to the hydropower system by equipment malfunction (right).....	16
Fig. 3.6 Fragility curves derived by Suppasri et al. (2013) for two-stories reinforced concrete buildings.	18
Fig. 3.7 Scatter plot depicting inundation depths and flow velocities simulated by a 2D model applied to the dam-break problem	19
Fig. 3.8 Fragility curves admitted for road infrastructure	19
Fig. 3.9 Map of damages to reinforced concrete buildings of two stories corresponding to a specific dam-break event. Adapted from Salzano et al. (2015).	20
Fig. 3.10 Map of damages to roads corresponding to a specific dam-break event. Adapted from Salzano et al. (2015).	20
Fig. 3.11 Inundation depth- steel strain relationships for the MRF 2-storey infilled building.....	23
Fig. 5.1 Structural configuration of Italian precast warehouses.....	30
Fig. 5.2 A schematic illustration of numerical model of a building with horizontal panels	31
Fig. 5.3 A schematic illustration of numerical model of a building with horizontal panels	33

List of tables

Table 3.1 Technology hazard matrix. 1: low - 4: high	9
Table 3.2 Parameters of the log-normal vulnerability functions to earthquakes (PGA). Specific for the conceptual dam system under study	15
Table 3.3 Parameters of the log-normal vulnerability functions to malfunctions. Specific for the conceptual dam system under study	17
Table 3.4 Parameters of the log-normal fragility curves admitted for road infrastructure. Have been admitted solely for the purpose of illustrating the methodology	19
Table 3.5 Definition of limit states for the different RC building typologies considered .	22
Table 3.6 Definition of limit states for the warehouse and the crane	22
Table 3.7 Parameters of fragility functions	24

***Europe Direct is a service to help you find answers
to your questions about the European Union.***

Freephone number (*):

00 800 6 7 8 9 10 11

(*) The information given is free, as are most calls (though some operators, phone boxes or hotels may charge you).

More information on the European Union is available on the internet (<http://europa.eu>).

HOW TO OBTAIN EU PUBLICATIONS

Free publications:

- one copy:
via EU Bookshop (<http://bookshop.europa.eu>);
- more than one copy or posters/maps:
from the European Union's representations (http://ec.europa.eu/represent_en.htm);
from the delegations in non-EU countries (http://eeas.europa.eu/delegations/index_en.htm);
by contacting the Europe Direct service (http://europa.eu/europedirect/index_en.htm) or
calling 00 800 6 7 8 9 10 11 (freephone number from anywhere in the EU) (*).

(*) The information given is free, as are most calls (though some operators, phone boxes or hotels may charge you).

Priced publications:

- via EU Bookshop (<http://bookshop.europa.eu>).

JRC Mission

As the science and knowledge service of the European Commission, the Joint Research Centre's mission is to support EU policies with independent evidence throughout the whole policy cycle.



EU Science Hub
ec.europa.eu/jrc



@EU_ScienceHub



EU Science Hub - Joint Research Centre



Joint Research Centre



EU Science Hub



Publications Office

doi:10.2788/10912

ISBN 978-92-79-64606-5